Fibroblast-Mediated Resistance to BRAF Inhibition in Metastatic Melanoma

Effect of drugs targeting PI3K/AKT/mTOR signaling pathway

Marta Gawraczynska

Master Thesis at the Department of Molecular Biosciences

Faculty of Mathematics and Natural Sciences

UNIVERSITY OF OSLO

June 2018

Fibroblast-Mediated Resistance to BRAF Inhibition in Metastatic Melanoma

Effect of drugs targeting PI3K/AKT/mTOR signaling pathway

Marta Gawraczynska

Master Thesis at the Department of Molecular Biosciences

Faculty of Mathematics and Natural Sciences

UNIVERSITY OF OSLO

June 2018

Fibroblast-Mediated Resistance to BRAF Inhibition in Metastatic Melanoma
Effect of drugs targeting PI3K/AKT/mTOR signaling pathway

Marta Gawraczynska

http://www.duo.uio.no/

Trykk: Reprosentralen, Universitetet i Oslo

Abstract

Introduction. Metastatic melanoma is an aggressive type of skin cancer for which the incidence rate has dramatically increased worldwide, especially in the Scandinavian countries. Targeted therapy with the BRAF inhibitor vemurafenib (BRAFi) has significantly improved clinical responses in melanoma patients carrying the *BRAF*^{V600} mutation. However, the clinical benefit is limited due to development of resistance. Recently, our group demonstrated that the presence of stromal cells, such as fibroblasts, can significantly influence melanoma sensitivity to BRAFi, indicating fibroblast-mediated protection from the drug. In this master project we investigated whether using a combination of BRAFi and drugs targeting PI3K/AKT/mTOR pathway could eliminate the fibroblast-mediated protection.

Methods. The drug sensitivity in two metastatic melanoma cell lines, HM8 and Melmet 5, was evaluated at different doses of selected inhibitors (BRAFi, CK2i, PI3Ki or mTORi). All inhibitors were used alone or with BRAFi combined with CK2i, PI3Ki or mTORi. First, the treatment effects on cell viability/proliferation were tested in melanoma mono-cultures. Subsequently melanoma cells were co-cultured with the fibroblast cell line WI-38, and treated with BRAFi alone or in combination with CK2i, PI3Ki or mTORi. Three different techniques, Western immunoblotting, Simple Western immunoassay and flow cytometry were used to investigate the levels of the phospho-proteins, pERK and pS6, reflecting the activity of the MAPK/ERK and PI3K/AKT/mTOR signaling pathways.

Results. The mono-cultured HM8 and Melmet 5 cells showed decreased cell viability with increasing concentrations of the mono-treatments. In addition, the BRAFi in combination with CK2i, PI3Ki or mTORi also reduced the melanoma cells' viability in mono-cultures. However, this reduction was mostly induced by the BRAFi. When HM8 co-cultures were treated with BRAFi, a lower sensitivity to this inhibitor was observed, indicating the fibroblast-mediated protection. The fibroblast-mediated protection was reduced or eliminated in co-cultures when the combination treatments of BRAFi with CK2i, PI3Ki or mTORi were used. Finally, the protein analysis revealed that BRAFi strongly reduced pERK and pS6 protein levels in the mono-cultures, and no additional effect was observed when BRAFi was combined with CK2i. In contrast, in the co-cultures, the effect of BRAFi on pERK and pS6 was lower and the combination treatment of BRAFi and CK2i further reduced the levels of these phospho-proteins.

Conclusions. The presence of fibroblasts protected melanoma cells from BRAFi. Combination treatment of BRAFi with drugs targeting PI3K/AKT/mTOR pathway, reduced/eliminated fibroblast-mediated protection. In the co-cultures, the BRAFi in combination with CK2i suppressed the MAPK/ERK and PI3K/AKT/mTOR signaling pathways more efficiently than BRAFi mono-treatment. In the mono-cultures, however, treatment with BRAFi was effective in suppressing both signaling pathways and the combination treatment with both inhibitors did not add any additional effect in suppression. This data suggest that combining BRAFi with PI3K/AKT/mTOR pathway inhibitors might overcome fibroblast-mediated protection and might be an attractive alternative for treating stroma-rich melanoma tumors.

Acknowledgement

The work presented in this master thesis was performed at the Department of Tumor Biology, Institute for Cancer Research, the Norwegian Radium Hospital, in the time period January 2017 to June 2018.

First of all, I would like to express my sincere gratitude to my main supervisor Dr. Mads H. Haugen, for giving me the opportunity to do my master thesis in the exciting field of melanoma. The door to your office was always opened whenever I had questions regarding my work and writing. You consistently allowed this master thesis to be my own work, but guided me in the right direction whenever you thought I needed it.

Secondly, I would like to thank my co-supervisor Dr. Lina Prasmickaite, for introducing me to this melanoma project and for sharing your knowledge with me. I am grateful for your time and your valuable comments, especially on the result part. Furthermore, I would also like to acknowledge the head of the department, Prof. Gunhild M. Mælandsmo, for letting me be a part of your research group. What is more, Prof. Fahri Saatcioglu, thank you for being my internal supervisor at the University of Oslo.

A very special gratitude goes out to my second co-supervisor Dr. Kotryna Seip. You have taught me more than I could ever give you credit for. Your patience in the laboratory, eye for perfection and constructive feedback have made this master project whole and successful. Your guidance and immense knowledge helped me at all the time of writing.

I am also so thankful to my friends and fellow students for dinners and events we shared for these last months. In addition, thanks to all members at the Department of Tumor Biology for a fantastic friendly working environment and technical question support.

Dear Mom and Dad, I want to express my gratitude for your care and continuous encouragement throughout my years of study. This master thesis would have not been possible without your unfailing support and motivation. You have always been there for me and taught me never give up. Words cannot describe how important you are to me. I also thank my little sister, Julia, for your childhood heart and for saying "I love you" when you woke up in the middle of the nights and I was still writing. This made me smile every time. In addition, thank you for the involuntary breaks you gave me while I wrote this thesis.

Finally, I would like to express my very profound gratitude to my beloved Sindre for being there for me, even though my mood was not always very optimistic. Thank you for all the laughter and conversations we shared during my master years. Also, thank you for being so supportive, although you did not always know what I was talking about. Yes, cancer is complicated! But most of all, thank you so much for believing in me.

Marta Gawraczynska
Oslo, May 2018

Abbreviations

AKT – Protein kinase B

AUC – Area under the curve

BRAF – Rapidly accelerated fibrosarcoma protein kinase B

BSA – Bovine serum albumin

CAF – Cancer associated fibroblast

CK2 – Casein kinase 2

CO_2 – Carbon dioxide

DMSO – Dimethyl sulfoxide

DNA – Deoxyribonucleic acid

DTT – Dithiothreitol

EC_{50} – Half maximal effective concentration

ECM – Extracellular matrix

EDTA – Ethylenediaminetetraacetic acid

ERK – Extracellular regulated kinase

FACS – Fluorescence-activated cell sorting

FBS – Fetal bovine serum

FDA – Food and drug administration

FSC – Forward scatter

GFP – Green fluorescence protein

HRP – Horseradish peroxidase

kDa – Kilodalton

MAPK – Mitogen-activated protein kinase

MEK – Mitogen-activated protein/extracellular signal-regulated kinase kinase

mTOR – The mechanistic/mammalian target of rapamycin

mTORC1 – The mechanistic/mammalian target of rapamycin complex 1

n – Number of biological replicates

NRAS – Neuroblastoma RAS viral oncogene homolog

PB – Pacific Blue

PBS – Phosphate-buffered saline

PI3K – Phosphatidylinositol-4,5-bisphosphate 3-kinase

PO – Pacific Orange

PTEN – Phosphatase and tensin homolog

PVDF – Polyvinylidene difluoride

RAF – Rapidly accelerated fibrosarcoma

RAS – Rat sarcoma

rpm – Revolutions per minute

RTK – Receptor tyrosine kinase

S6 – Ribosomal protein S6

S6K – Ribosomal protein S6 kinase

SEM – Standard error of mean

SSC – Side scatter

St.dev. – Standard deviation

TME – Tumor microenvironment

UV – Ultra violet

X

Table of Contents

1. Introduction

1.1. Cancer

Cancer is a broad group of diseases characterized by abnormal cell growth and their potential to invade and spread from the site of origin (primary site) to other sites in the body[1]. Such uncontrollably cells' division and growth leads to the formation of solid mass of tissue, called a tumor. A benign tumor, also known as non-invasive, lacks the ability to invade surrounding tissue or metastasize. Contrarily, a malignant tumor, also known as invasive, can spread into surrounding tissue and metastasize.

Cancer is among the leading causes of death globally. The World Health Organization has reported 8,8 million cancer-related deaths worldwide in 2015[2], the same year there were 10 944 deaths from cancer in Norway[3]. In 2016, almost 33 000 Norwegians were diagnosed with cancer[3]. The latest worldwide cancer statistics estimated that the incidence and cancer-related deaths numbers are expected to be doubled during the next fifteen years[4]. The expected increase in both numbers could be partly caused by aging and enlarged number of the population, as the risk of cancer usually increases significantly with age, as well as an increased exposure to risk factors such as smoking, physical inactivity, alcohol, ultraviolet (UV) radiation, reproductive changes and infectious agents[4].

In 2011, Hanahan and Weinberg have defined eight hallmarks of cancer and two enabling characteristics essential for cancer development and progression[5]. They proposed that sustaining proliferative signaling, evading growth suppressors, avoiding immune destruction, enabling replicative immortality, activating invasion and metastasis, inducing angiogenesis, resisting cell death and deregulating cellular energetics are the eight universal hallmarks important during carcinogenesis (Figure 1.1)[5]. In addition, tumor-promoting inflammation and genome instability and mutation are suggested to be the two enabling characteristics that make it possible for the cells to acquire cancer hallmarks.

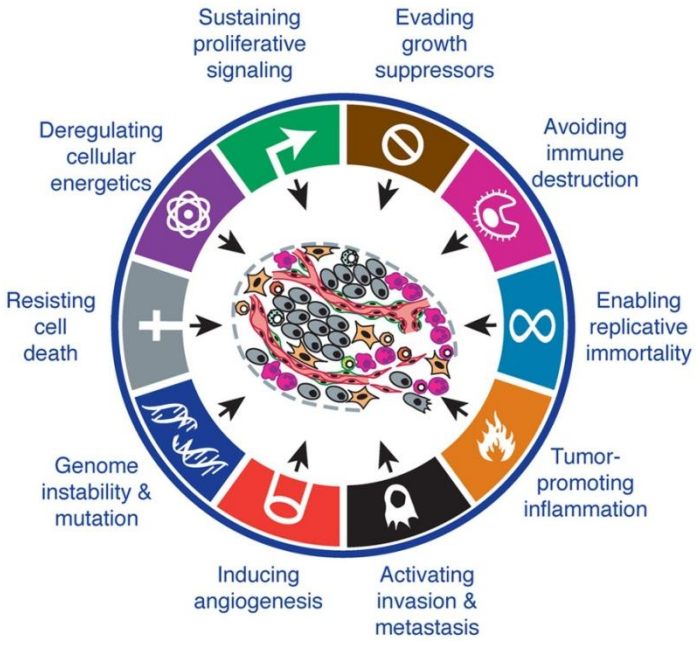

Figure 1.1: General hallmarks of cancer. Schematic representation of the eight hallmarks and two enabling characteristics of cancer essential for tumor development and progression, proposed by Hanahan and Weinberg. Modified and reproduced with permission from Elsevier [5].

1.1.1. Cancer genes

The critical genes responsible for cancer development and progression can be classified in two groups, the tumor-suppressor genes and oncogenes. Tumor-suppressor genes encode proteins that regulate uncontrolled or abnormal proliferation, stimulate apoptosis and are involved in DNA-repair processes[6]. Inactivated by mutations tumor-suppressor genes lose or reduce the function of the gene product, which can lead to selective growth advantage to the neoplastic cell and cancer progression[7]. For example, *p53* gene (*TP53*) is a tumor-suppressor gene that encodes the tumor protein p53 (p53), which regulates cell growth and proliferation, in addition to stimulate the apoptosis. Mutations in *TP53* gene (e.g. point mutations), present in approximately 50% of all melanoma, inactivates p53 protein and may lead to uncontrolled cell division and growth[8, 9].Proto-oncogenes are normal genes that due to mutations or increased expression can become activated oncogenes. For example, mutations in *BRAF* oncogene (e.g. point mutations) are frequently observed in melanoma patients[10]. *BRAF* gene encodes the protein BRAF (serine/threonine protein kinase), which activates and regulates the MAPK/ERK signaling pathway[11]. Mutated proto-oncogenes may give a cell an increased advantage of uncontrolled cell proliferation and the ability to resist apoptosis, which in turn contributes to cancer formation[8, 12]. Tumor-suppressor genes and oncogenes have a key role in induction and progression of cancer. Importantly, these genes are associated to cancer

hallmarks i.e. concerned to abnormalities in cell proliferation and resisting apoptosis linked to formation of cancer.

1.1.2. Metastasis

Metastasis is the process by which neoplastic cells spread from their primary site of origin to distant locations in the body[7]. Until now it still remains as the major cause of 90% of cancer-associated deaths from solid tumors[12, 13]. Development of metastasis can occur even after many years after diagnosis of the primary tumor[14].

Metastasis involves a complex, multi-step process where all stages must be successfully completed to give a rise to a metastatic tumor (Figure 1.2)[15]. In order to metastasize, cancer cells need to break away from the well-confined primary tumor and degrade proteins that form the basement membrane and extracellular matrix (ECM). During local invasion, cancer cells secrete various proteases, such as metaloproteases, that can breach the basement membrane[16]. The step of local invasion is necessary for further intravasation into the lumina layer of nearby blood vessels. After successful intravasation, the carcinoma cells have to survive the hemodynamic shear forces and avoid detection by the immune system in the bloodstream[17]. The surviving cancer cell can be arrested in the circulation and then extravasate the blood vessel at the distant site[18]. During the final stages of invasion-metastasis cascade, tumor cells must survive in the foreign microenvironment and form metastasis. Due to the fact that the microenvironment of invaded normal tissue parenchyma is unlike that existing in the site of primary tumor, malignant cells must adapt to the new environment in order to be able to proliferate and colonize in the distant site. The newly arrived cancer cells may enter a state of dormancy[19], where they are in quiescent state until the right micro-environmental conditions appear. Dormant cells may later in life become activated and start their proliferation, this may clarify metastases appearing even several years after successful treatment of the primary tumor[17, 19].

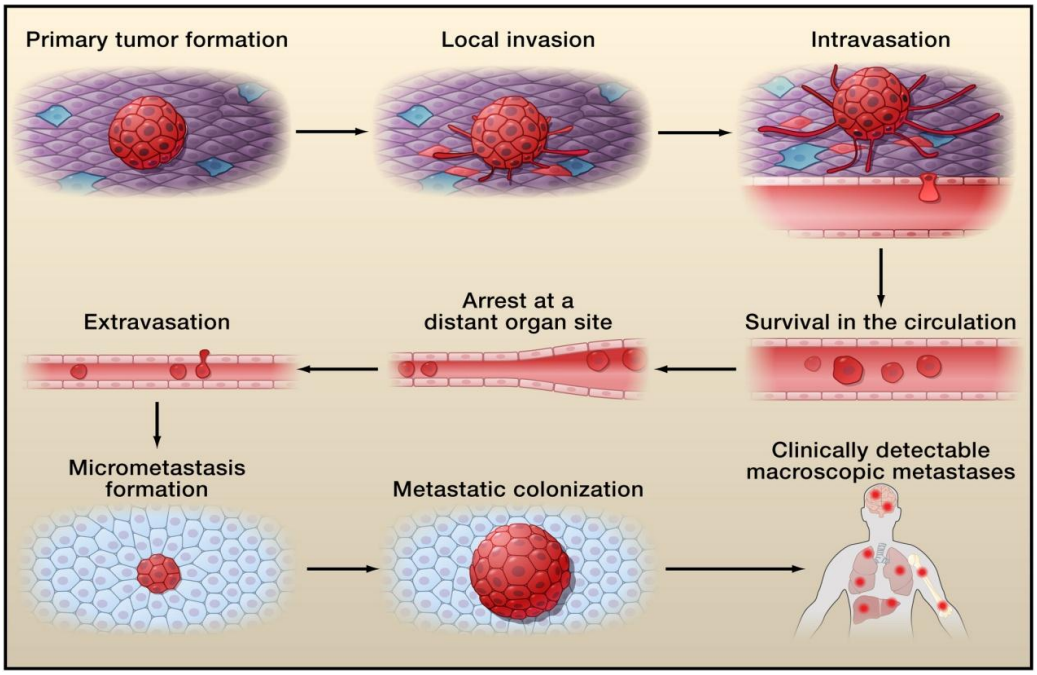

Figure 1.2: The main steps of the invasion-metastasis cascade. Clinically detectable metastases characterize the successful formation of metastatic tumor by carcinoma cells undergoing the invasion-metastasis cascade. Reproduced with permission from Elsevier [17].

Clinical observations maintain that metastasis is in some measure site-directed[13]. Though, this observation is not new and has already been introduced as the "*Seed and Soil*" theory by Stephen Paget back in the 19th century[20]. Based on this theory cancer cells ("seeds") metastasize to preferential organs ("soil"), depending on the primary cancer type. The most frequent organs for the metastasis to occur are the lymph nodes, lungs, liver, brain and the bones. In the case of e.g. breast cancer, the metastases are frequently established in the lungs or bones[21]. Skin cancer type, melanoma, can establish metastases in many different organs e.g. lymph nodes, liver, lungs, brain or skin[13, 22].

1.1.3. Cancer associated signaling

The mitogen-activated protein kinase (MAPK)/extracellular regulated kinase (ERK) pathway and phosphatidylinositol-3-kinase (PI3K)/Protein kinase B (AKT)/mechanistic target of rapamycin (mTOR) pathway are the signaling pathways which are constitutively activated, dysregulated and involved in the activation of various cancer types, including melanoma (Figure 1.3)[23-25]. Both signaling pathways are essential in melanoma developing and progression, making them to important therapeutic targets[26].

The MAPK/ERK is a complex pathway activated in all melanomas by the ligand binding (e.g. growth factors, mitogens, cytokines or hormones) to the transmembrane protein, receptor tyrosine kinase (RTK)[27]. The dimerization of RTK triggers the activation of the GTPase (small G protein), RAS. Activated RAS interacts and activates the protein kinase BRAF, which phosphorylates second protein kinase, MEK. The cascade in turn phosphorylates the third protein kinase, ERK[27]. The successful activation and phosphorylation of the downstream elements in the MAPK/ERK cascade lead to translocation of ERK to the nucleus, where the various transcription factors can be activated. This pathway regulates the genes responsible for cell proliferation, differentiation and survival[26].

The PI3K/AKT/mTOR pathway is activated by upstream signaling of RTK which in turn activates serine/threonine kinase AKT[28]. The activated AKT initiates a cascade of downstream signaling events, including mTOR complex 1 (mTORC1)[29], an important component in the regulation of cell growth and proliferation[30]. The mTOR phosphorylates and activates the ribosomal protein S6 kinase, S6K[25]. Ribosomal protein S6 (S6), is phosphorylated by S6K and can acts as an indicator of mTOR activation[31].

Casein kinase 2 (CK2) is involved in regulation of the MAPK/ERK and PI3K/AKT/mTOR signaling pathways and increases cell proliferation, cell growth and cell survival[32-34]. CK2 can act on PI3K, directly phosphorylate AKT or phosphorylate ERK[35, 36]. However, the general role of this serine/threonine kinase is poorly understood and described in the literature[33].

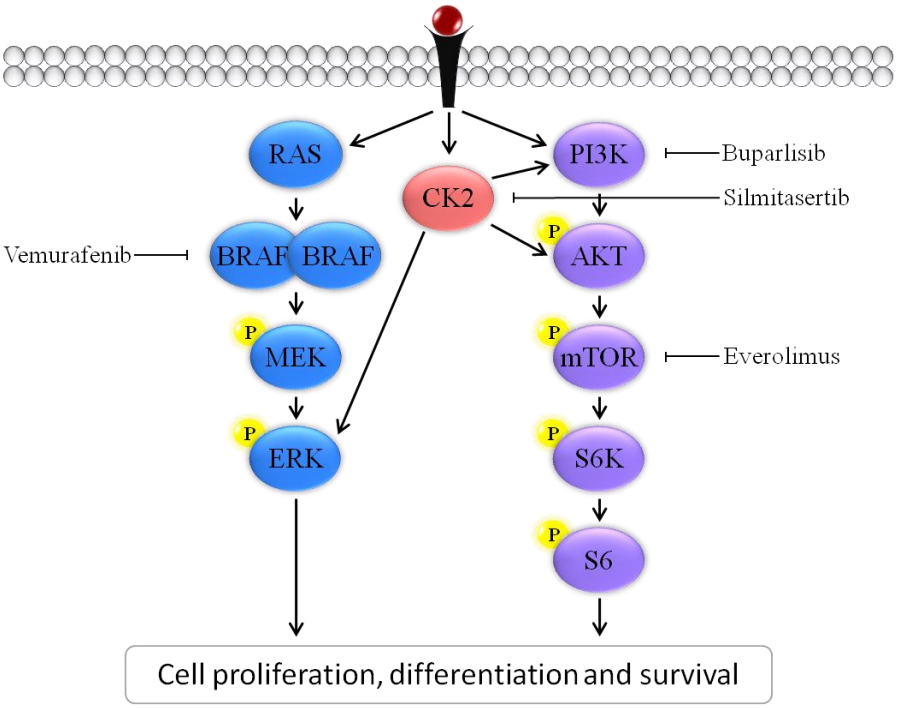

Figure 1.3: A simplified overview of the cancer associated MAPK/ERK and PI3K/AKT/mTOR signaling pathways. The ligand binding initiates a cascade of downstream signaling events in both pathways. The inhibitors of BRAF, CK2, PI3K and mTOR are indicated in the figure.

1.2. Tumor microenvironment

The tumor microenvironment (TME) is the environment that surrounds the tumor. TME generally consists of surrounding blood and lymphatic vessels, immune cells, neuroendocrine and adipose cells, fibroblasts, signaling molecules and the extracellular matrix (ECM)[37]. TME has an essential role in the development and progression of malignant tumor[38], for example by the formation of new blood vessels (angiogenesis) and the foundation of the optimal environment for the tumor growth[39]. The angiogenesis is crucial for sufficient supply with nutrients and oxygen to the neoplasm expansion. Extracellular signals released by the tumor and soluble factors (such as growth factors, chemokines and cytokines) released by the stromal cells can influence the microenvironment and affect the tumor formation. The secreted signals can contribute to the growth and survival of the neoplastic cells, as well as the migrations of these cells into the TME[40, 41]. In addition, soluble factors can mediate cell-cell communication between the cells in the microenvironment. TME is highly involved in the response to therapeutic treatment, and stromal cells (e.g. fibroblasts) have the ability to induce resistance to targeted drugs[42].

1.2.1. Cancer associated fibroblasts

Fibroblasts are one of the most abundant stromal cell types in TME[43]. One of their functions is to synthesize the proteins of ECM as well as various soluble factors. Fibroblasts have also an important role in tissue homeostasis and wound healing[43]. During neoplastic progression, fibroblasts are reprogrammed into cancer associated fibroblasts (CAFs). CAFs are the essential components of the TME in carcinogenesis and can be beneficial to the cancer cells[44, 45]. For example, various growth factors, cytokines and chemokines released from CAFs were shown to contribute to cancer proliferation and invasion[46, 47]. CAFs regulatory factors secreted into the TME are important in contribution to therapy resistance[45]. Furthermore, CAFs' ability to degrade ECM proteins facilitates the angiogenesis, that can result in increase of tumor mass and metastasis[48, 49]. CAFs are the potential molecular targets for cancer treatment, inhibition of CAFs interactions with tumor and TME can potentially lead to the suppression of tumor development and growth[45].

1.3. Melanoma

Melanoma is an aggressive type of skin cancer that originates in the melanocytes[50]. Melanocytes are the cells producing the melanin pigment. These cells can be located predominantly in the bottom layer of skin's epidermis (Figure 1.4), iris in the eyes and hair follicles[51]. Melanin pigment is mainly responsible for skin colour and is also involved in protection against ultraviolet (UV) radiation. However, melanocytes can also be injured and transformed by UV leading to malignant transformation[52]. Approximately 90% of all melanoma cases occur on the skin, called cutaneous melanoma, this is the most common type of melanoma[53].

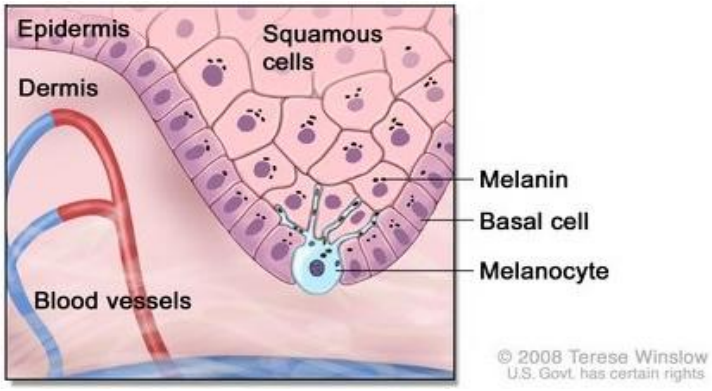

Figure 1.4: Anatomy of the skin with melanocytes. The melanocytes are located in the basal cell layer of the epidermis. The melanin is present in the squamous cells of the epidermis. For the National Cancer Institute © 2008 Terese Winslow LLC, U.S. Govt. has certain rights.

1.3.1. Epidemiology

The incidence of melanoma has dramatically increased worldwide[54]. In the Scandinavian countries this disease is counting 4% of all cancers and is responsible for approximately 2% of all cancer-related deaths[55]. In 2016, 2 114 Norwegians were diagnosed with malignant melanoma[3]. The incidence rate is highly affected by race and geographic location[53]. Some phenotypic characteristics, such as lighter pigmentation, red hair or numerous freckles (common among Caucasians), can give increased risk of developing malignant disease[53, 54]. The incidence rate of this disease also increases with age and mostly young (25-49 years) and middle-aged people (>50 years) are affected[54]. The major environmental risk factor for developing malignant melanoma is the exposure to UV radiation from sun and tanning beds[54, 56]. Furthermore, family history of melanoma or numerous nevi are the other risk factors that can contribute to development of melanoma, since the pigmentation pattern is extremely heritable[54, 57].

1.3.2. Stages of melanoma progression

The American Joint Committee on Cancer (AJCC) has developed the system for classification of the main I-IV stages for melanoma based on the Tumor (T), Node (N) and Metastasis (M) categories[58]. The internationally standard TNM classification describes the primary tumor size (T), the regional lymph node involvement (N) and the absence or presence of metastatic spread (M). The TNM categorization into stages is crucial to appropriate treatment and individual prognosis for patients with cutaneous melanoma[59]. In stage I and II, the tumor is located in the skin and there is no regional involvement of lymph nodes or distant metastases. In stage III, one or more lymph nodes are affected and the regional metastasis can occur. The presence of distant metastases to other organs is characteristic in stage IV[60].

The melanoma progression is a stepwise process of normal melanocytes transformation toward malignant melanoma (Figure 1.4). The MAPK/ERK pathway mutations (e.g. *BRAF*^{V600E} mutation) can initiate abnormal proliferation of melanocytes resulting in benign nevus formation. Further mutations and progression of structural atypia lead to the development of dysplastic nevus. During radial-growth phase the lesions can proliferate intraepidermally. Progression from the radial-growth phase to the vertical-growth phase is characterized by the cells' ability to penetrate the basement membrane and enter dermis. In

the final phase, the cancer cells can invade the blood and lymphatic system and metastasize to distant organs[61].

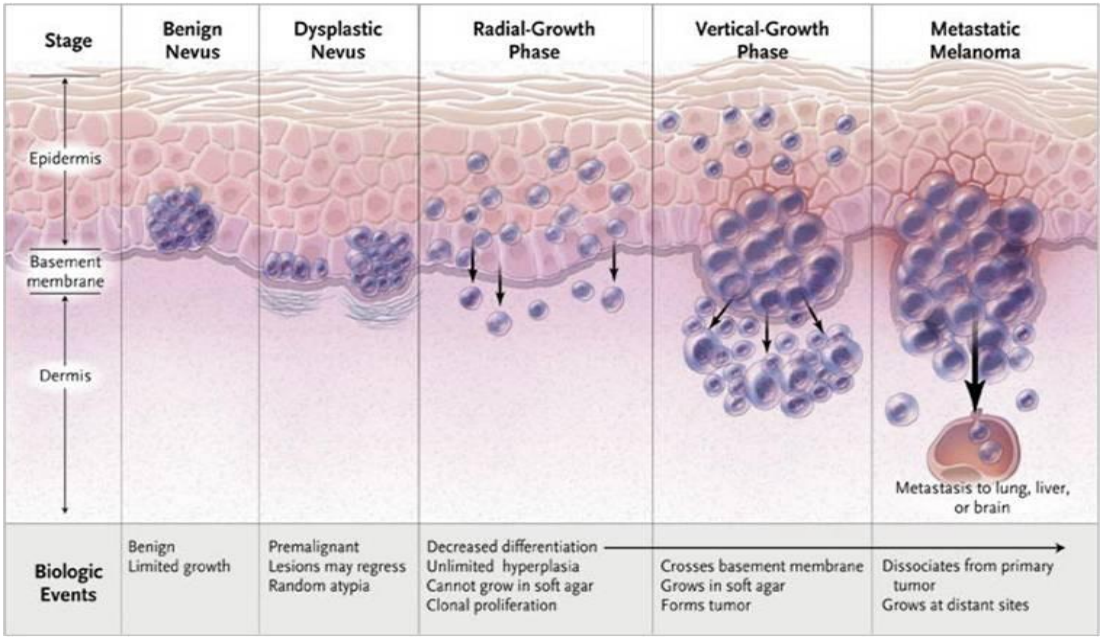

Figure 1.4: Stages and biological events in the progression of melanoma. The progression from normal melanocytes to metastatic melanoma is a multistep process. A benign nevus is formed when the melanocytes undergo uncontrolled growth. The further mutations induce the dysplastic nevus phase, characterized by the abnormal size, multiple colors, irregular borders and increased surface. During radial-growth phase the cells can invade the local epidermis, while in the vertical-growth phase the cells can cross the basement membrane. The successful spread to distant organs (lymph nodes, lungs, liver or brain) occurs in the last metastatic melanoma phase. Modified and reproduced with permission from [61], Copyright Massachusetts Medical Society.

1.3.3. BRAF mutations

The mutations in genes involved in the MAPK/ERK pathway can affect the cells' normal proliferation, growth and survival[62, 63]. The *BRAF* gene encodes the BRAF protein kinase, an important component in the MAPK/ERK pathway. *BRAF* mutations are observed in approximately 50% of melanomas[11], while the *NRAS* mutations are present in 15-20% of cutaneous melanomas[64]. The most common *BRAF* mutation is the single substitution of valine to glutamic acid at position 600 ($BRAF^{V600E}$), which account for 80% of the cutaneous melanoma cases[65]. $BRAF^{V600E}$ mutation leads to increased activation of downstream elements in the MAPK/ERK signaling pathway, which drives the tumor development[62]. This mutation is frequently involved in sun-exposed skin[66]. The other less common *BRAF* mutations are V600K and V600R that represents 20% and 7% of *BRAF* mutants, respectively[63].

1.3.4. Treatment of malignant melanoma

The early detection of melanoma is possible to treat with surgery and can significantly improve the mortality[66]. The surgical treatment is the most effective option at an early stage of tumor progression (stage I and II), before the spread of the tumor to other organs. In 2011, the Food and Drug Administration (FDA) has approved treatment with the BRAF inhibitor vemurafenib (also known as PLX4032) of late-stage melanoma, when the metastatic occurs[66]. The median survival of patients with advanced or metastatic melanoma is 6 to 10 months[67]. The treatment with oral drug vemurafenib, specific for the *BRAF*^{V600E} mutation, has improved the median survival of patients to approximately 16 months[67]. Other less frequent V600 mutations are also sensitive to treatment with the BRAF inhibitor vemurafenib[11]. The targeted therapy with vemurafenib inhibits the MAPK/ERK signaling pathway by binding to monomers of BRAF mutated kinases (Figure 1.3)[68]. The inhibition of BRAF mutants results in decreased cell proliferation, in addition to blocking the spread and progression of the malignant tumor[69].

1.4. Drug resistance

Targeted therapy with the BRAF inhibitor vemurafenib has shown improved clinical responses in advanced or metastatic melanoma patients carrying the *BRAF*^{V600} mutation. However, the therapeutic benefit is limited due to resistance developing occurring within 6 to 8 months of mono-treatment initiation[63, 70]. Development of the resistance mechanisms, such as intrinsic and acquired resistance[71], gives the neoplastic cells' ability to tumor progression and growth. The intrinsic resistance is observed when no clinical response is achieved in melanoma patients during and after treatment with BRAF inhibitor, while the acquired resistance occurs when relapse or progression of disease is observed after clinical benefit[63]. The intrinsic resistance mechanisms that allows melanoma cells to escape targeting are the loss of PTEN[72], as well as the mutations in genes upstream of RAF, *BRAF* and *NRAS*[73]. The reactivation of the MAPK/ERK pathway is the main mechanism of acquired resistance to BRAF inhibitors, present in approximately 70% of resistant tumors[74, 75]. The activation of the alternative proliferation-inducing PI3K/AKT/mTOR signaling pathway is proposed to be an additional mechanism of acquired resistance development, present in 22% of resistant and progressive cases[73].

The development of resistance suggests that inhibition of one target in the signaling pathway may be ineffective in blocking the tumor progression[76]. The resistance development in BRAF-mutant melanomas remains an important challenge to overcome and is under clinical investigation. Different signaling pathways are involved in melanoma progression and growth. The combination treatment with drugs targeting several pathways or molecules is an attractive alternative for therapy of melanoma, which may potentially overcome or prevent resistance to BRAF inhibition[77]. Further discovery of new therapeutic targets will also improve the treatment of melanoma patients resistant to clinically available inhibitors.

Aims of the study

The interactions between tumor cells and stromal cells in the tumor microenvironment (TME) can influence tumor response to therapy. Previously, our group has shown that malignant melanoma cells co-cultured with stromal cells, i.e. fibroblasts, have reduced sensitivity to the BRAF inhibitor vemurafenib (BRAFi), indicating fibroblast-mediated protection from this drug. The main aim of this master thesis was to evaluate the effects of the PI3K/AKT/mTOR signaling inhibitors with the goal to overcome fibroblast-mediated protection from BRAFi. The secondary aims were:

- Map the sensitivity of two melanoma cell lines grown as mono-cultures to the PI3K inhibitor buparlisib (PI3Ki), CK2 inhibitor silmitasertib (CK2i) and mTOR inhibitor everolimus (mTORi) alone and in combination with BRAFi.

- Investigate and compare the effect of BRAFi alone and BRAFi in combination with PI3Ki, CK2i or mTORi in melanoma-fibroblast co-cultures.

- Evaluate the effect of BRAFi and CK2i alone and in combination on the levels of phosphorylated ERK and S6 as indicators of the activity of MAPK/ERK and PI3K/AKT/mTOR signaling, respectively.

2. Materials and methods

2.1. Cell lines

In this thesis two metastatic melanoma cell lines, HM8 and Melmet 5, and one stromal cell line, human lung fibroblasts WI-38 (table 2.1), have been used in the *in vitro* studies.

The metastatic melanoma cell lines were established from the biopsies of metastatic melanoma patients at the Department of Tumor Biology, the Norwegian Radium Hospital. The isolated tumor cells were cultured as monolayer, as described in chapter 2.1.1. The lung fibroblasts WI-38 were bought from American Type Culture Collection (ATCC). The cell line was derived from normal embryonic lung tissue from a Caucasian female.

Table 2.1: Summary of the background information regarding metastatic melanoma cell lines and stromal cell line used in this thesis.

Name	Tissue of origin	Received from
HM8	Brain metastasis	Norwegian Radium Hospital, Norway
Melmet 5	Lymph node metastasis	Norwegian Radium Hospital, Norway
WI-38	Lung	ATCC, Manassas, VA

2.1.1. Cell culturing

Tumor cells and stromal cells were grown as mono-cultures or co-cultures. For mono-cultures, HM8 and Melmet 5 cell lines were grown as a monolayer in tissue-culture flasks in RPMI-1640 medium supplemented with 10% fetal bovine serum (FBS) and 2mM L-Alanyl L-Glutamine, further referred as RPMI++. Fibroblasts were grown as a monolayer in EMEM medium, containing 2nM L-Alanyl L-Glutamine and supplemented with 10% FBS. In order to investigate an effect of tumor microenvironment on tumor cells, co-culture experimental model was used, where melanoma cells were cultured together with fibroblasts as monolayer in RPMI++ medium. The growing cells were kept in incubator holding stable temperature at 37 °C and a constant CO_2 level of 5%.

2.1.2. Cell subculturing

The cells were kept under observation daily using a light microscope. Under sterile conditions cells were subcultured approximately 2-3 times per week, once the cell' confluence reached approximately 85-90%. Briefly, the cells were rinsed twice with phosphate-buffered saline (PBS) buffer and incubated with the ethylenediaminetetraacetic acid (EDTA) (for melanoma cells) or 0,25% Trypsin-EDTA solution (for fibroblasts and co-cultures) for 3-5 minutes, resulting in detachment of the cells. The detached cells were collected in a 15 mL tube and centrifuged at 1000 rpm for 5 minutes. After centrifugation, a supernatant was removed and a desired amount of cell suspension was transferred to a new flask containing fresh medium (pre-heated in advance in a water bath at 37 ºC) for further culturing.

2.1.3. Cell counting

Countess™ II Automated Cell Counter was used for live cells counting and viability measurements. To count cell viability, trypan blue stain was used. The 10 µL of cell suspension was mixed with 10 µL of trypan blue stain (ratio 1:1) and inserted into a Countess™ cell counting chamber slide. The trypan blue staining will selectively penetrate the pores in the membrane of non-viable cells (dead or dying cells) and colour them blue, while the viable cells (the cells with intact cell membrane) will not be permeable for uptake of dye. The Countess™ II automated cell counter can then quickly determinate the accurate viable cells number in the used cell suspension.

2.1.4. Cell freezing

To prepare frozen cell stocks, the cells that have reached a confluence of approximately 85-90% were rinsed, detached with the EDTA or 0,25% trypsin-EDTA solution, collected and counted as described above under chapters 2.1.2. and 2.1.3. The cells were then mixed with a freezing medium, containing 50% cell culturing medium, 40% FBS and 10% DMSO, and freezed overnight at -80 °C by using the CoolCell® cell freezing container. A day after cells were transferred to a liquid nitrogen tank for indefinite storage.

2.1.5. Cell thawing

Frozen cells from the liquid nitrogen tank were rapidly thawed in a 37 °C water bath and diluted slowly by using pre-warmed growth medium. To remove remaining toxic DMSO, the cell suspension was centrifuged at 1000 rpm for 5 minutes followed by a removal of the supernatant. The cells were then re-suspended in a fresh pre-heated medium and transferred into a tissue-culture flask at a high density to ensure a better cell' recovery. When the cells reached the confluence of 85-90% they were split for further culturing and experimental use.

2.1.6. *In vitro* drug testing

To evaluate drug effects on cancer cells' viability, cells were seeded into 96-well plate and incubated for 24 hours. For mono-culture treatment the cancer cells were seeded out at a density of 7000 cells/well for HM8 and 6000 cells/well for Melmet 5. For co-culture treatment the cells were seeded out at a ratio of 1:5 (HM8/Melmet 5:WI-38). After 24 hours incubation, the cells were treated either with one drug (mono-therapy), or a combination of two drugs (combination therapy, where one of the drugs was always BRAFi). For all experiments, inhibitors were diluted in the RMPI++ medium to get the desired concentrations. The control cells were treated with DMSO, equivalent to the highest dose of the drug (all drugs dissolved in DMSO), to ensure that DMSO alone does not affect cell viability. The plates were incubated under normal culturing conditions for 72 hours. At the end of the treatment, cell viability was determined by measuring bioluminescence as described in the chapter 2.2.1.

2.1.7. Cell preparation for protein analysis

The cancer cells were grown as mono-cultures or co-cultures in T25 tissue-culture flasks. For mono-cultures, the cancer cells were seeded out at a density of 700 000 cells/flask for HM8 and 600 000 cells/flask for Melmet 5 in 5 mL RPMI++ medium. For co-cultures, cells were seeded out at a ratio of 1:5 (HM8/Melmet 5:WI-38) to reach a final density of 700 000 cells/flask in 5 mL RPMI++ medium. After 48 hours incubation, the cells were treated with either mono-therapy or combination therapy for the next 24 or 48 hours, depending on the experimental set-up. The cells were then detached with the EDTA (for melanoma cells) or 0,25% Trypsin-EDTA solution (for fibroblasts and co-cultures), collected and washed twice with PBS.

- *Cell lysates*

Cell pellets were lysed for 30 minutes by lysis buffer (see supplementary table for recipe), containing protease and phosphatase inhibitors to prevent protein degradation and dephosphorylation, respectively. To further disrupt the cells' membrane, sonication was applied to the cells for 5-10 seconds at +4 °C. The lysates were then centrifuged at 13000 rpm for 15 minutes in a cold room (+4 °C). The supernatant containing proteins was collected and the protein concentration was determined (see chapter 2.3.1.). The cell lysates were stored at -80 °C for further use.

- *FLOW samples*

Cell pellets were re-suspended in 200 µL of Pacific Blue (PB) dye diluted in PBS to a final concentration of 0,0375 ng/µL and incubated in the dark at 4 ºC for 15 minutes. PB penetrates the cell membrane only of dead cells which eventually can be separated by FLOW cytometry. Further, cells were centrifuged at 1000 rpm for 5 minutes, washed twice with a PBS and fixed in 1.6% paraformaldehyde solution (400 µL per 1 million cells) for 10 minutes at room temperature. After incubation, the cells were centrifuged at 2000 rpm for 5 minutes and permeabilized in ice cold 100% methanol (MeOH) (500 µL per 1 million cells) at -20 ºC for at least 10 minutes before usage or kept at -80 °C for a long storage.

2.1.8. Drugs

Multiple targeted drugs have been used in this thesis (Table 2.2). Vemurafenib (BRAFi), silmitasertib (CK2i) and buparlisib (PI3Ki) were purchased from Selleck Chemicals. Everolimus (mTORi) was from Novartis. All drugs were dissolved in DMSO.

Table 2.2: Overview of therapeutic drugs overview, stock concentrations and concentrations used in this thesis.

Drug name	Stock concentration	Concentrations used	Target
Vemurafenib (BRAFi)	20 mM	0,1-5 µM	BRAF
Silmitasertib (CK2i)	20 mM	0,1-20 µM	CK2
Buparlisib (PI3Ki)	10 mM	0,1-10 µM	pan-PI3K
Everolimus (mTORi)	20,88 mM	0,1-20 nM	mTOR

2.2. Cell viability measurement

2.2.1. Bioluminescence assay

The bioluminescence assay measures the production and emission of light by living cells. The luciferase enzyme and luciferin substrate are both essential in the bioluminescent reaction, where the chemical energy is converted into light energy. During this chemical reaction, the luciferin is oxidized by the luciferase and can then produce an excited state molecule that emits light, bioluminescence. It was also previously shown that the emitted light signal intensity corresponds to the proportional number of living cancer cells[78].

At the department of Tumor Biology at the Norwegian Radium Hospital, both melanoma cell lines HM8 and Melmet 5 were previously stable transfected with a gene expressing luciferase. D-luciferin at the final concentration of 0,1mg/mL was added to the cells and incubated in a dark at room temperature for 10 minutes before a measurement was made by a Victor™ *X*3 Multimode plate reader. White walls and clear bottoms 96-well plates were used in all experiments.

2.3. Protein analysis

Several different techniques are available to study proteins. The Western immunoblotting, Simple Western system and FLOW cytometry have been used in this thesis and explained in more details below in chapters 2.3.2., 2.3.3. and 2.3.4.

2.3.1. Protein concentration measurement

The protein concentration in cell lysates was measured by using the Pierce™ BCA Protein Assay Kit containing BCA Reagent A, BCA Reagent B and albumin standard (2 mg/mL). This assay kit is based on the reduction of Cu^{+2} to Cu^{+1} by protein in an alkaline solution. The purple-colored reaction product exhibits an absorbance at 562 nm, which is nearly linearly with increasing protein concentrations.

2 µL of cell lysates were mixed with 18 µL of PBS per well in a 96-well plate. Two technical parallels were made for each sample. 20 µL per well of the albumin standard at 6 concentrations (1 µg/µL, 0,5 µg/µL, 0,25 µg/µL, 0,125 µg/µL, 0,063 µg/µL and 0 µg/µL) was

applied into a plate. Each well was supplemented with 150 µL of reagent A and reagent B mixture (ratio 50:1) and incubated for 20 minutes in the dark. Absorbance was measured at 595 nm by Victor™ *X*3 Multimode plate reader. The protein concentrations were calculated by using the albumin calibration curve.

2.3.2. Western Immunoblotting

Western immunoblotting is a commonly used semi-quantative, antibody-based analytical technique for separation and identification of specific proteins in a homogenate sample. During gel electrophoresis the proteins are separated based on their molecular size (kDa). The proteins are then transferred onto polyvinylidene difluoride (PVDF) membrane by using an electrical gradient. The antibodies are specific, they bind to the protein of interest and observable band/bands can be detected on the membrane. The thickness of the band/bands represents the amount of the protein present in a sample.

2.3.2.1. Sample preparation

20 µg of the cell lysates were mixed with a loading buffer, reducing agent and pure water to a total volume of 20 µL. The samples were then incubated on a heater plate at 75 °C for 5 minutes to disrupt the hydrogen bonds between the molecules in the samples. After the incubation time, the samples were spun down and placed on ice until being used.

2.3.2.2. NuPAGE Bis-Tris gel electrophoresis

The NuPAGE® 4-12% Bis-Tris 1,0 mm 12 well gel was prepared by removing the comb and the tape. The wells were washed with distilled water and the gel was placed in an electrophoresis chamber. The inner chamber was filled with a 1x MES running buffer (suitable to separate small to medium sized proteins) up to the brim of the chamber, while the outer chamber was filled half-way with the same buffer. The denatured samples were loaded into the gel, 20 µL per well. A SeeBlue® Pre-Stained standard, consisting of known size proteins, was also loaded into a gel as a molecular weight marker. The electrophoresis was started with a voltage of 125V. Soon after the samples have moved slightly downwards toward the anode (positive pole), the voltage was increased up to 150V and run for another 60-90 minutes.

2.3.2.3. Transfer of the proteins

The proteins from the gel were transferred onto a PVDF membrane in a semi-dry transfer. The membrane was activated (pre-wet) in 100% MeOH in fume hood and rinsed several times with distilled water. The gel was released from a frame and the construction of the "sandwich" in XCell II™ Blot Module was made in this order: 2x sponges, whatman paper, gel, PVDF membrane, whatman paper, 1x sponge, 3x whatman papers and 2x sponges. The prepared Blot Module construction was inserted into a western blot chamber and filled with a transfer buffer (see supplementary table for recipe), while the outer chamber was filled with cold water. The instrument was set to 400mA and run for 60 minutes. After completed run, the PVDF membrane was released from the blot module and the ladder was marked with a pen for later visualization.

2.3.2.4. Immunodetection

To reduce non-specific binding, the PVDF membrane was blocked with 10% BSA-TBST buffer (see supplementary table for recipe) for 60 minutes. The membrane was then incubated overnight at +4 °C with the primary antibody diluted in 5% BSA-TBST buffer (see Table 2.3 for more details). Three time washing steps with TBST buffer (10 minutes each) followed in order to remove all unbounded antibody from the membrane. The secondary horseradish peroxidase (HRP)-tagged antibody diluted in 5% BSA-TBST buffer was added and the membrane was further incubated at room temperature for another 60 minutes. The last three washing steps with TBST buffer (10 minutes each) followed before protein detection was performed.

Table 2.3: Primary and secondary antibodies used for immunodetection on Western blots.

Primary antibody	Size (kDa)	Blocking, in TBST	Dilution of 1. Ab	Secondary antibody	Dilution of 2. Ab
pERK	42/44	5% BSA	1:2000	Rabbit	1:3500
pS6	32	5% BSA	1:2000	Rabbit	1:3500
Total ERK	42/44	5% BSA	1:1000	Rabbit	1:3500
Total S6	32	5% BSA	1:1000	Rabbit	1:3500
Histone 3	17	5% BSA	1:2000	Rabbit	1:5000

2.3.2.5. Visualization of the membrane

The membrane was placed into a luminescent detection G:Box (Syngene™) instrument. The Super Signal West Dura kit solution was applied on the membrane. The mix has reacted with HRP-labeled secondary antibodies and the chemiluminescence (light emission) was measured. The development was done by using the GeneSnap software (version 7.12).

2.3.3. Simple Western system

Protein Simple© has revolutionized the classical protein detection method, the Western immunoblotting, to a new Peggy Sue instrument. The simple western system is a useful method allowing a capillary electrophoresis-based separation and analyzes of proteins by their size or charge ranging from 2-440 kDa in size, where only a small sample volume is needed. In this master thesis only a size-based analyze has been performed and, therefore, described exclusively in more details below.

The simple western analysis is initiated when the capillaries are loaded with stacking and separation matrices, before the denatured protein lysates are taken up by the machine (Figure 2.1). An electric voltage through the capillaries is then induced resulting in protein separation and detection along the separation matrix. In order to immobilize the proteins to capillary walls, ultraviolet (UV) light illumination is used. This protein fixation step is followed by a blocking step, which prevents from unspecific antibodies binding. Appropriate primary and HRP-labeled secondary antibodies are loaded before luminol-peroxide mix is applied to the capillaries. The mix reacts with HRP-labeled secondary antibodies. This reaction produces a bioluminescence signal which is proportional to protein levels and can be presented as an electropherogram by using the Compass software. The amounts of proteins in the samples can be then determinated by calculating the area under the curve (AUC).

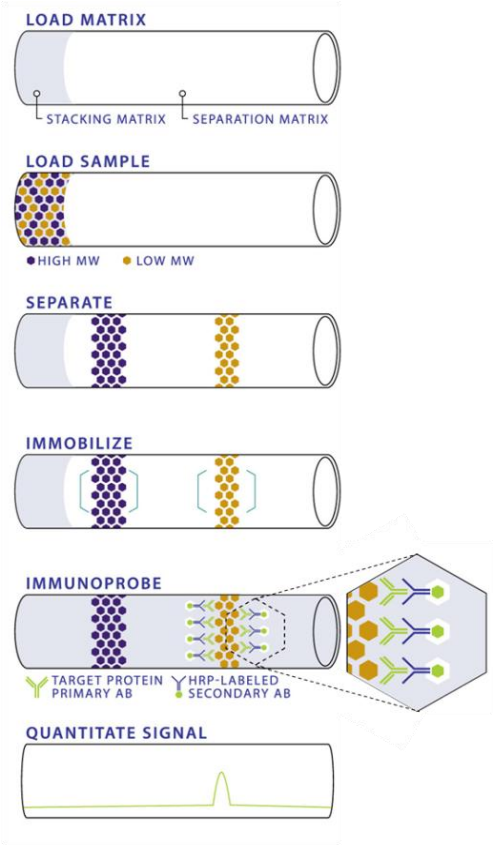

Figure 2.1: Schematic overview of size-based Simple Western immunoassay. Multiple steps of the Simple Western immunoassay are indicated in the figure (ProteinSimple™).

2.3.3.1. Standard pack reagents preparation

Compounds from the standard pack, including biotinylated ladder, 5x Fluor Master and Dithiothreitol (DTT), provided by the ProteinSimple™, were prepared as follows:

- DTT was dissolved in 40 µL of deionized water making a final solution of 400 mM.
- The 5x Fluor Master was dissolved in 20 µL of 10x Sample buffer (provided by the ProteinSimple™) and 20 µL of prepared 400 mM DTT solution.
- The biotinylated ladder was dissolved in 16 µL of deionized water, 2 µL of 10x Sample buffer and 2 µL of prepared 400 mM DTT solution.

2.3.3.2. Sample preparation

All samples to a final volume of 5 µL/well were supplemented with the 5x Fluorescent Master Mix (contains three fluorescent proteins that normalize the distance for each independent capillary) at a ratio of 1:4 and further, if necessary, diluted with deionized water in order to

obtain the recommended protein concentration of 0,8 mg/mL. The samples were then denatured at 95 °C for 5 minutes, vortexed, spun down and stored on ice.

2.3.3.3. Preparation of the antibodies

The primary antibodies used for the simple western immunoassay were diluted with an Antibody Diluent II (provided with a kit) at different dilutions as indicated in Table 2.4. The secondary HRP-tagged antibodies were provided by the producer and used as it is. Both the primary and secondary antibodies were used in a final volume of 15 µL/well.

Table 2.4: Primary and secondary antibodies used for immunodetection on Simple Western.

Primary antibody	Dilution	Secondary antibody
pERK	1:50	Rabbit
pS6	1:200	Rabbit
β-actin	1:150	Rabbit

2.3.3.4. Mix Luminol-S and peroxide

Luminol-Peroxide Mix was prepared by mixing 100 µL of Luminol-S with 100 µL of peroxide. The mix was vortexed and placed on ice.

2.3.3.5. Pipetting the assay plate

The pre-heated (95 °C, 5 min.) biotinylated ladder (5 µL), prepared samples (5 µL), Antibody Diluent II (20 µL), primary antibodies (15 µL), streptavidin-HRP (15 µL), secondary antibodies (15 µL), Luminol-Peroxide Mix (15 µL), deionized water (30 µL), separation and stacking matrixes (both 15 µL) were loaded into the 384-well microplate, as represented in Figure 2.2. The prepared microplate was centrifuged at 2500 rpm at room temperature for 5 minutes to ensure that no air bubbles were present in the wells. Remaining air bubbles were removed with a needle, if needed, before inserting the plate into the instrument.

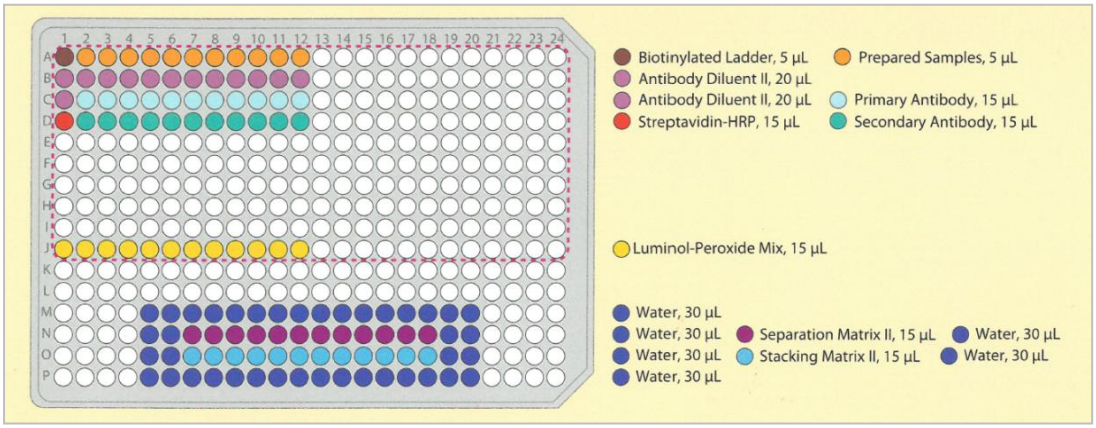

Figure 2.2: The illustration of 384-well assay microplate used in Simple Western immunoassay experiments (ProteinSimple™).

2.3.3.6. Handling the Peggy Sue instrument

By selecting the start button in the program, further instructions for preparation and setup of the instrument were followed. The waste reservoir was emptied and the water reservoir was filled on the auxiliary module. A new sponge was placed in the manifold wash station. Wash buffer (30 mL), running buffer (20 mL), matrix removal buffer (20 mL) and capillary box were inserted into the accurate positions on the resource tray. The lid-covered assay microplate was placed on the sample tray. The settings for the experiment were predefined in the Compass program and the run was initiated. The incubation time with primary antibody was setup to 60 minutes, while the incubation time with secondary antibody was setup to 30 minutes. The results were analysed by the Simple Western software "Compass" (version 3.1.7).

2.3.4. FLOW cytometry

Flow cytometry is a laser-based technique for analyzing up to thousands of particles per second, such as cells. This method is often used for cell counting, cell sorting or detection and quantification of biomarkers. In a flow cytometer machine, the cells suspended in a liquid stream are passed through a laser light beam and a scattered light from the cells is detected. A photodetector in front of the light beam measures forward scatter (FSC) that is proportional to the size of the cell and several detectors to the side measure side scatter (SSC) that is proportional to the shape and internal complexity of the cell. Flow cytometry can also by using fluorescence detectors detect emitted light from excited fluorescent molecules, such as

fluorescent labeled antibodies, or fluorescent dyes or stains. The flow cytometer instrument measures the voltage pulse for each single event and the events number correspond to the number of cells detected. Overall, FLOW cytometry allows simultaneous multiparametric analysis of the cells.

2.3.4.1. Sample barcoding

In order to eliminate sample-to-sample staining variation four samples were barcoded. To do so, 3-5 x 10^5 cells of each sample were washed twice with 1 mL PBS and centrifuged at 2000 rpm for 5 minutes before the cells were re-suspended in different concentrations (0 µg/mL, 0,04 µg/mL, 0,2 µg/mL, 2 µg/mL) of Pacific Orange (PO) dye. Cells were incubated in a dark at room temperature for 30-60 minutes and eventually washed with 1 mL PBS containing 1% bovine serum albumin (BSA). After centrifugation at 2000 rpm for 5 minutes cells were re-suspended in 200 µL of 1% BSA-PBS and all four barcoded samples were pulled together into one tube. To insure that an excess of PO is completely washed, cells were centrifuged at 2000 rpm for 5 minutes once more.

2.3.4.2. Sample staining with antibodies

PO-stained cells were divided into two tubes at ratio 1:3. The sample with the fewer cells was kept unstained while the sample with more cells was stained with both pERK-PE (1:50 dilution in 1% BSA-PBS) and pS6-Alexa 647 (1:200 dilution in 1% BSA-PBS) antibodies simultaneously in a dark at room temperature for 30-60 minutes. After the incubation the cells were washed with 1% BSA-PBS, centrifuged at 2000 rpm for 5 minutes before the cells' re-suspension in 400 µL of 1% BSA-PBS.

2.3.4.3. Compensation control preparation

Compensation controls are required for multiparameter FLOW cytometry to ensure that the observed detection of increased signal intensity of the protein of interest is not due to the spilover by any other used fluorochromes in the assay, such as a signal from the barcoding, live-dead cell dye or any other combined fluorochromes.

- *Pacific Orange compensation*

To prepare PO compensation control, 3 x 10^5 of non GFP-tagged HM8 cells were washed with 1 mL PBS and centrifuged at 2000 rpm for 5 minutes before being divided into four

groups and stained with different concentrations of PO (0 µg/mL, 0,04 µg/mL, 0,2 µg/mL, 2 µg/mL) in a dark at room temperature for 30-60 minutes. After the incubation, the cells were washed with 1% BSA-PBS and centrifuged at 2000 rpm for 5 minutes before pulling all differently stained cells together in 500 µL of 1% BSA-PBS.

- *GFP compensation*

To prepare GFP compensation control, 1,5 x 10^5 of non GFP-tagged and 1,5 x 10^5 of GFP-tagged HM8 cells were mixed together, washed with 1 mL PBS and centrifuged at 2000 rpm for 5 minutes (this step was repeated twice). The cells were re-suspended in 500 µL of 1% BSA-PBS.

- *Antibody compensation*

To prepare PE and Alexa 647 compensation controls, 3 x 10^5 of non GFP-tagged HM8 cells were washed with 1 mL PBS and centrifuged at 2000 rpm for 5 minutes (this step was repeated twice) before the cells were stained with either PE- or Alexa 647-labelled antibodies (both diluted 1:100 in 1% BSA-PBS) in a dark at room temperature for 30-60 minutes. After the incubation, the cells were washed with 1% BSA-PBS, centrifuged at 2000 rpm for 5 minutes before the cells were re-suspended in 500 µL of 1% BSA-PBS.

2.3.4.4. Cell gating strategy

For cell analysis, a subsequent gating of the cells was performed as illustrated in Figure 2.3. FSC and SSC parameters have been used for detection of the main cell population. SSC width (SSC-W) against SSC area (SSC-A) further allowed a separation of single cells from duplets. Dead cells were then separated from live cells based on the intensity of Pacific Blue dye in the cells (stained prior-cell fixation). Eventually, cell discrimination by GFP signal intensity against Pacific Orange dye intensity was performed in order to identify four different samples. GFP^+ tumor cells were then analysed for different fluorescence signals such as Alexa 647 and PE.

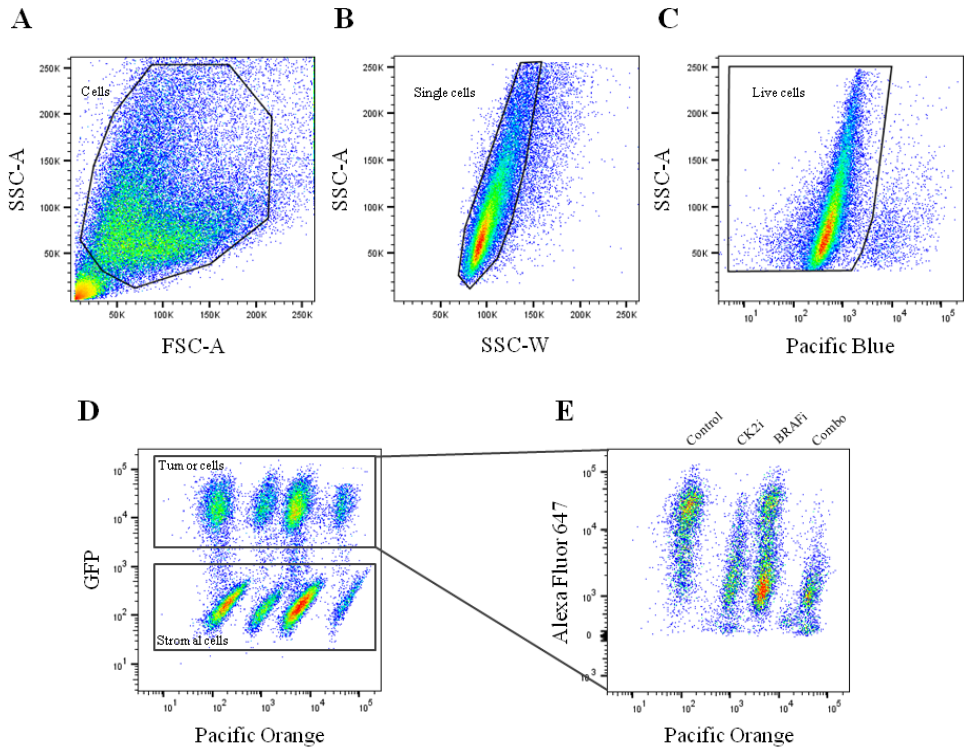

Figure 2.3: Illustration of cell gating strategy used in the flow cytometry analysis. Samples were analysed by sequential gating where first cells from debris were distinguished (A); then single cells were separated from doublets (B); and only live single cells (C) were further analysed for GFP signal intensity, where GFP^+ cells are recognized as tumor cells and GFP^- cells are recognized as stromal cells (D). At last, level of protein of interest in GFP^+ tumor cells was analysed (E).

2.3.4.5. Data acquisition

All experiments were performed on LSR II FLOW cytometer. Just before the run all the samples were filtrated to prevent the instrument from clogging and run one by one for a short time on low speed in order to adjust all necessary instruments' parameters. Compensation controls were recorded first, 1 x 10^5 events from each control, followed by the manually performed compensation. For each unstained and stained sample of interest 1-3 x 10^5 events were recorded. Data analyses were performed by using the FlowJo software (version 10.3).

2.4. Data and statistical analysis

In this study, the data obtained from each experiment was statistically analysed by using the Microsoft® Excel software. In all experiments the treated samples were normalized to the non-treated samples (controls). When an experiment was performed once or twice ($n \leq 2$), an average and standard deviation (st.dev.) were calculated. When an experiment was performed three or more times ($n \geq 3$), an average and standard error of the mean (SEM) were calculated. The statistical significance was analysed by using Student's t-test, which determinates the significance difference between the set of data. The statistical level of significance (p-value) is marked with asterisks throughout the thesis and set to less or equal to 0.05 in all represented results.

The half maximal effective concentration (EC_{50}), which is the concentration of drug inducing 50% of the maximum response in mono-cultures, was estimated from the drug concentration response curves. First, the drug concentrations were Log2 transformed by using the Microsoft® Excel software. The linear equation $y = mx + c$, where y was set to the value equal of the half of maximum drug effect, m and c were constants determined from the curve and the value of x representing the EC_{50} was determined.

3. Results

3.1. Sensitivity of melanoma cells grown as mono-cultures to selected targeted drugs

To evaluate drug sensitivity in two metastatic melanoma cell lines, HM8 and Melmet 5 cells labeled with GFP-luciferase were treated with different doses of selected targeted drugs. In this thesis, BRAF inhibitor vemurafenib (BRAFi), CK2 inhibitor silmitasertib (CK2i), PI3K inhibitor buparlisib (PI3Ki) and mTOR inhibitor everolimus (mTORi) were used. The melanoma cells' response to targeted drugs (Figure 3.1) was analysed by measuring bioluminescence produced by luciferase-expressing cells, as described in the chapter 2.2.1.

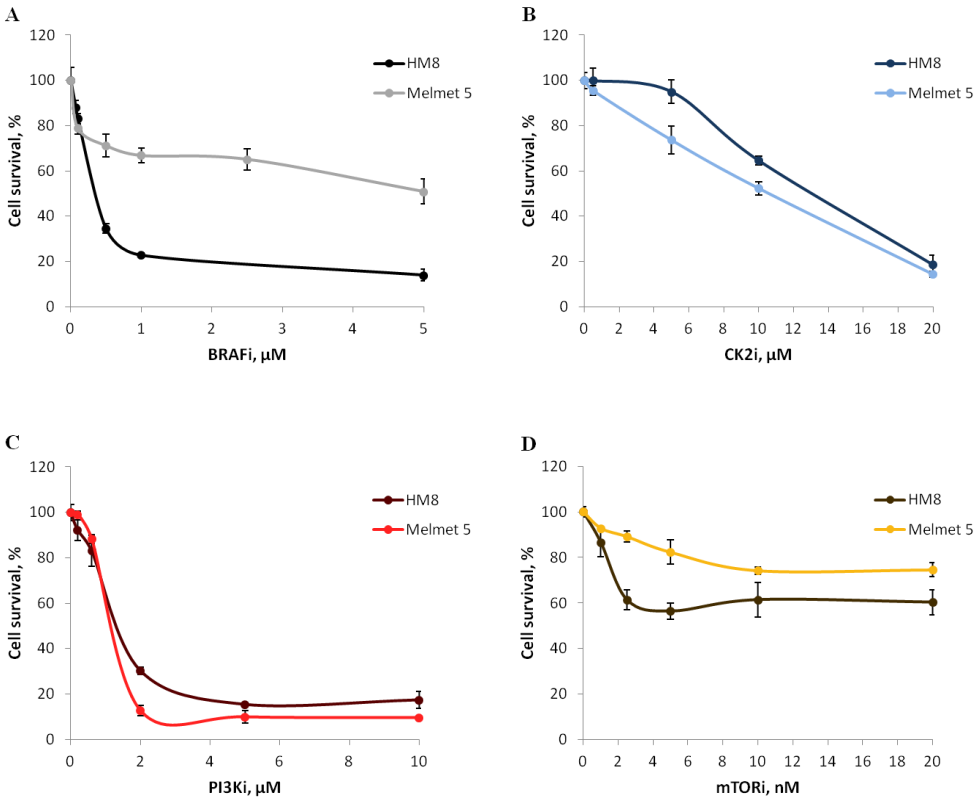

Figure 3.1: Drug sensitivity in two melanoma cell lines. The melanoma cell lines HM8 and Melmet 5 grown as mono-cultures were treated with different doses of BRAFi (A), CK2i (B), PI3Ki (C) and mTORi (D) for 72 h before the cell viability was scored by measuring bioluminescence. The effect is presented as % relative to the non-treated controls for each cell line. Error bars indicate standard deviations (st.dev.) from 3 technical parallels.

The dose response data were used to estimate the half maximal effective concentration (EC_{50}) which is the concentration inducing 50% of the maximum response, after 72 h treatment. As seen from Table 3.1, HM8 cells were more sensitive to BRAFi and mTORi, while Melmet 5 cells were more sensitive to CK2i. The response to PI3Ki was relative similar in both cell lines.

Table 3.1: Half maximal effective concentration (EC_{50}). EC_{50} values for the HM8 and Melmet 5 cells grown as mono-cultures.

Drug	HM8 cell line	Melmet 5 cell line
BRAFi	0,41 µM	1,16 µM
CK2i	7,86 µM	5,23 µM
PI3Ki	1,04 µM	1,09 µM
mTORi	2,50 nM	5,43 nM

Looking more specific into each dose response we observed that HM8 and Melmet 5 cell lines showed decreased cell viability with increasing BRAFi concentrations, indicating the cell lines' general sensitivity to this drug (Figure 3.1 A). A dose of 0,5 µM, which was later selected as the most optimal dose, resulted in 66% and 29% reduction in cell viability in HM8 and Melmet 5, respectively. Thus, at this dose the HM8 sensitivity to the BRAFi was greater than Melmet 5, and it remained so with increasing concentrations of the drug. In contrast, at low concentrations of CK2i, HM8 was less sensitive to the drug than Melmet 5 (Figure 3.1 B). For example, a dose of 10 µM resulted in 35% and 48% reduction in cell viability in HM8 and Melmet 5, respectively. However, a dose of 5 µM appeared to have a little effect on both cell lines. PI3Ki induced a very effective reduction in cell viability in HM8 and Melmet 5, indicating a high sensitivity to PI3Ki in both cell lines (Figure 3.1 C). A dose of 0,6 µM has reduced the cell viability to 88% in HM8 and 83% in Melmet 5. Both melanoma cell lines were treated with PI3Ki doses up to 10 µM, but there was no additional reduction in cell viability by increasing the dose above 5 µM, which already led to low cell survival. At low concentrations of mTORi, Melmet 5 was less sensitive to the drug than HM8 (Figure 3.1 D). A dose of 5 nM, later selected as the most optimal dose, resulted in 44% and 13% reduction in cell viability (in HM8 and Melmet 5, respectively), indicating a differences in sensitivity to the drug between these two cell lines. Both cell lines were treated with mTORi doses up to 20 nM, but there was no additional effect by increasing the dose above 10 nM.

3.2. Sensitivity of melanoma cells grown as mono-cultures to the combination treatment

To evaluate the effect of combination treatment on HM8 and Melmet 5 cell lines, different concentrations of BRAFi were combined with various concentrations of CK2i, PI3Ki and mTORi.

All the tested doses of CK2i in a combination with all BRAFi doses gave a decrease in cell viability when compared to BRAFi mono-treatment (Figure 3.2 A). The observed decrease in cell viability indicates also that the combination treatment was more effective in cell viability reduction compared to CK2i mono-treatment.

The Melmet 5 cells responded to the combination treatment with decreased cell viability (Figure 3.2 B). Mono-treatment with CK2i was very effective in reducing cell viability. However, no additional effect in cell viability reduction was observed when the BRAFi was added at the doses of 2,5 or 5 µM of CK2i, compared to BRAFi mono-treatment.

Altogether, the HM8 and Melmet 5 cells' response to the combination treatment with BRAFi and CK2i was primarily induced by the effect of BRAFi.

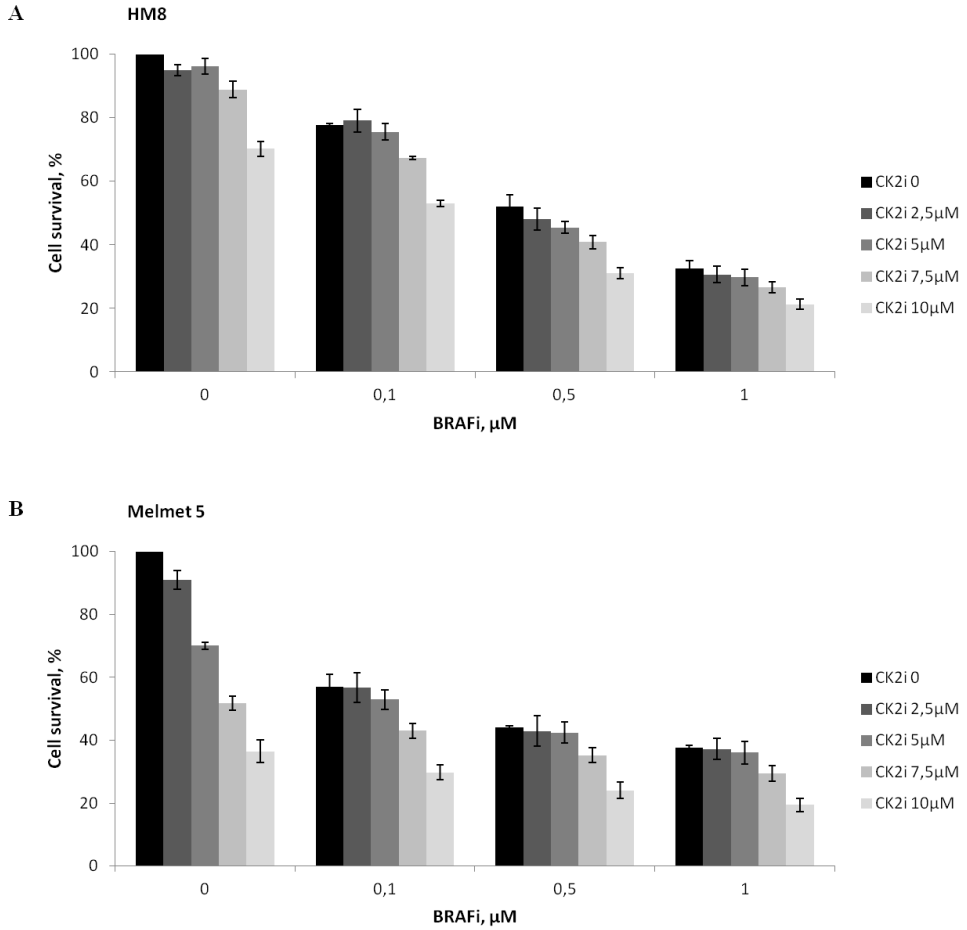

Figure 3.2: Drug sensitivity response in melanoma cells treated with BRAFi and CK2i combined. Melanoma cell lines HM8 (A) and Melmet 5 (B) grown as mono-cultures were treated with different doses of BRAFi in a combination with different concentrations of CK2i for 72 h. The cell viability effect on melanoma cells was scored by measuring bioluminescence and is presented as % relative to the non-treated controls. Data presents average ± SEM, $n \geq 3$.

The combination treatment with BRAFi and PI3Ki on HM8 and Melmet 5 cells decreased cell viability compared to BRAFi and PI3Ki mono-treatments (Figure 3.3). However, mono-treatment with either BRAFi or PI3Ki was very effective in reducing cell viability in both cell lines. The HM8 and Melmet 5 cells' response to the combination treatment with BRAFi and PI3Ki was mostly induced by the effect of BRAFi.

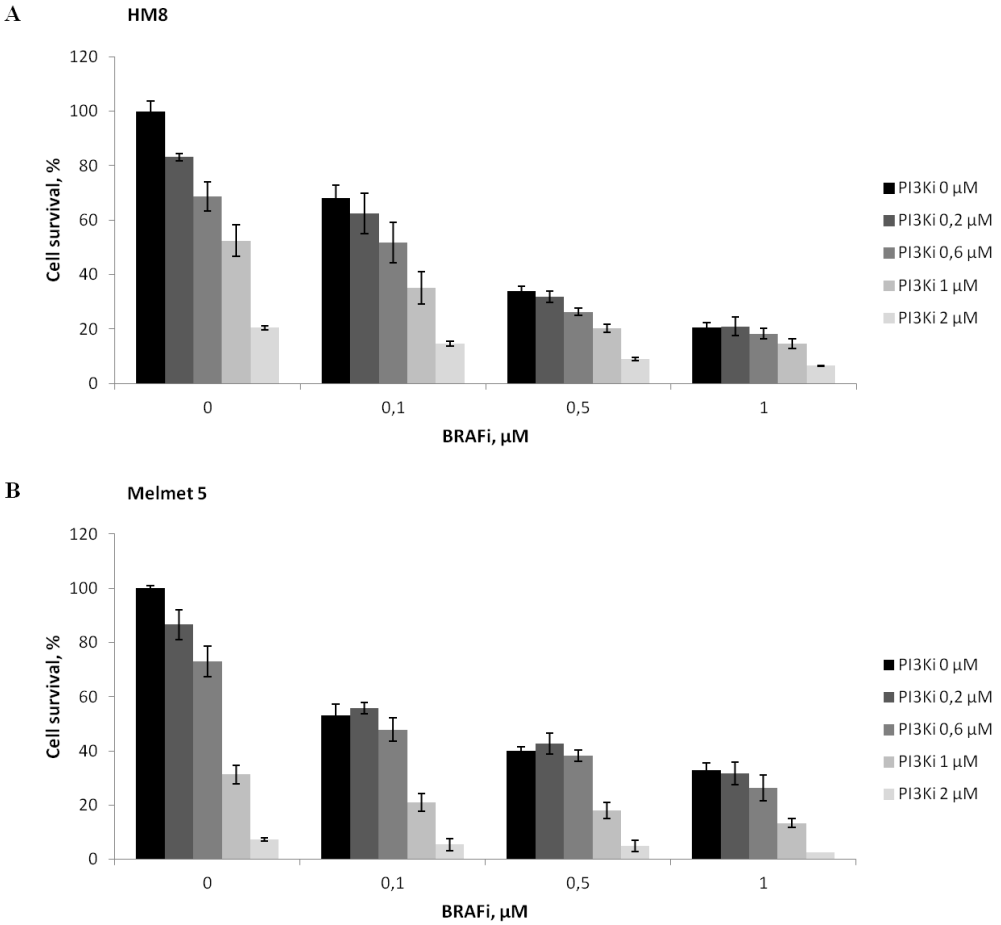

Figure 3.3: Drug sensitivity response in melanoma cells treated with BRAFi and PI3Ki combined. Melanoma cell lines HM8 (A) and Melmet 5 (B) grown as mono-cultures were treated with different doses of BRAFi in a combination with different doses of PI3Ki for 72 h. The cell viability effect on melanoma cells was scored by measuring bioluminescence and is presented as % relative to the non-treated controls. Error bars indicate st.dev. from 3 technical parallels.

The HM8 cells' response to the combination treatment with BRAFi and mTORi was not more effective in cell viability reduction than BRAFi mono-treatment (Figure 3.4 A). However, the results implied that the combination treatment with selected drugs decreased cell viability compared to mTORi mono-treatment.

The combination treatment with BRAFi and mTORi of Melmet 5 cells decreased cell viability, compared to mono-treatment with mTORi in all tested concentrations (Figure 3.4 B). Mono-treatment with mTORi was not effective in reducing cell viability. However, no additional effect in viability reduction was observed when the BRAFi was combined with mTORi, compared to BRAFi mono-treatment.

Overall, the HM8 and Melmet 5 cells' response to the combination treatment with all selected drugs was primarily induced by the effect of BRAFi.

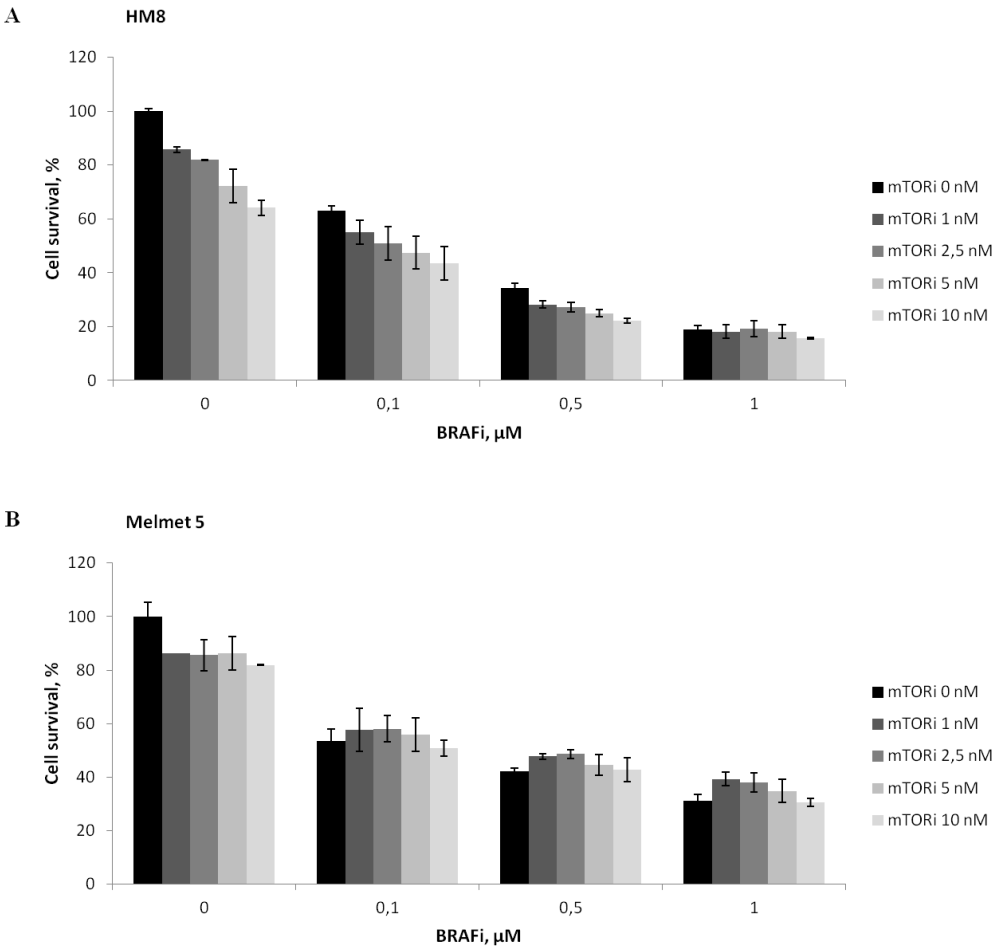

Figure 3.4: Drug sensitivity response in melanoma cells treated with BRAFi and mTORi combined. Melanoma cell lines HM8 (A) and Melmet 5 (B) grown as mono-cultures were treated with different doses of BRAFi and mTORi for 72 h. The cell viability effect on melanoma cells was scored by measuring bioluminescence and is presented as % relative to the non-treated controls. Error bars indicate st.dev. from 3 technical parallels.

3.3. Lung fibroblasts mediate protection and reduce melanoma cells' sensitivity to BRAFi

The presence of lung fibroblasts can significantly reduce the melanoma cells' response to BRAFi, as previously published by the group[78]. To confirm whether the presence of stromal cells alters the melanoma cells' response to BRAFi, HM8 cells were grown either as mono-cultures or co-cultures with the lung fibroblasts WI-38, and treated with increasing doses of BRAFi.

Viability of the HM8 cells was decreased by 60% after 72 hours of BRAFi treatment in the absence of fibroblasts. However, viability of the cancer cells was decreased only by 20% in the presence of fibroblasts (Figure 3.5). This indicates a lower sensitivity to the BRAFi of the HM8 cells when grown in co-cultures with lung fibroblasts.

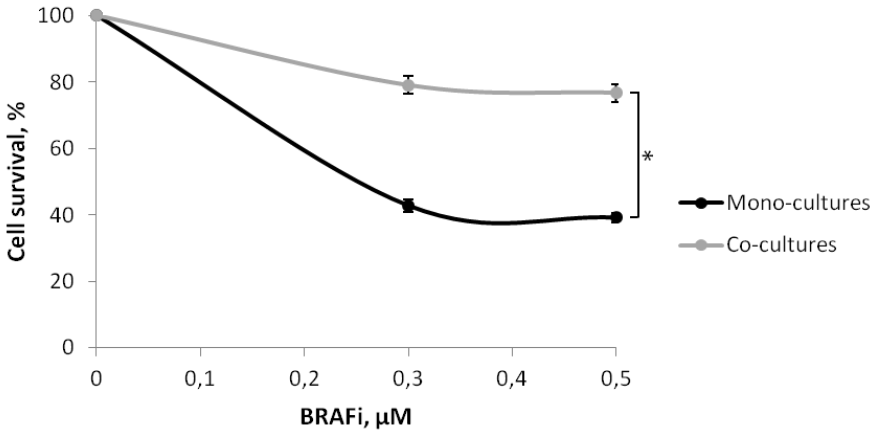

Figure 3.5: Melanoma cells co-cultured with lung fibroblasts are more resistant to BRAFi. HM8 cell line grown as a mono-culture or co-culture with lung fibroblasts WI-38 with/without BRAFi treatment for 72 h. The effect on melanoma cells was scored by measuring bioluminescence and is presented as % relative to the non-treated controls (average ± SEM, $n \geq 3$). *, p-value < 0,05, unpaired t-test.

These results signify that presence of fibroblasts reduce sensitivity of HM8 cells to BRAFi and underline the importance of identifying other targeted drugs, or a combination treatment, that eliminates the fibroblasts-mediated protection in melanoma cells.

3.4. Comparison of mono treatment versus combination treatment of melanoma cells

In order to investigate if the fibroblast-mediated protection of melanoma cells from BRAFi (Figure 3.5) can be reduced or eliminated, the combination treatments were tested. The cancer cells were grown as mono- and co-cultures and treated with the BRAFi, combined with CK2i, PI3Ki or mTORi. Mono-treatments with all tested drugs were applied for comparison.

The results indicated that fibroblasts-associated cancer cells' resistance to BRAFi in co-cultures was reduced with the combination treatment of BRAFi and CK2i for both melanoma cell lines (Figure 3.6). The cell viability was approximately 80% in HM8 co-cultures treated with BRAFi or CK2i mono-treatment, while with the combination treatment the cell viability decreased to 45%. The cell viability of Melmet 5 grown as co-cultures was above 45% when treated with mono-treatment of BRAFi or CK2i, but decreased to 31% with the combination treatment of both targeted drugs.

Altogether, this indicated that the protection induced by the stromal cells was reduced in HM8 cells and completely abolished in Melmet 5 cells when BRAFi was used in a combination with CK2i.

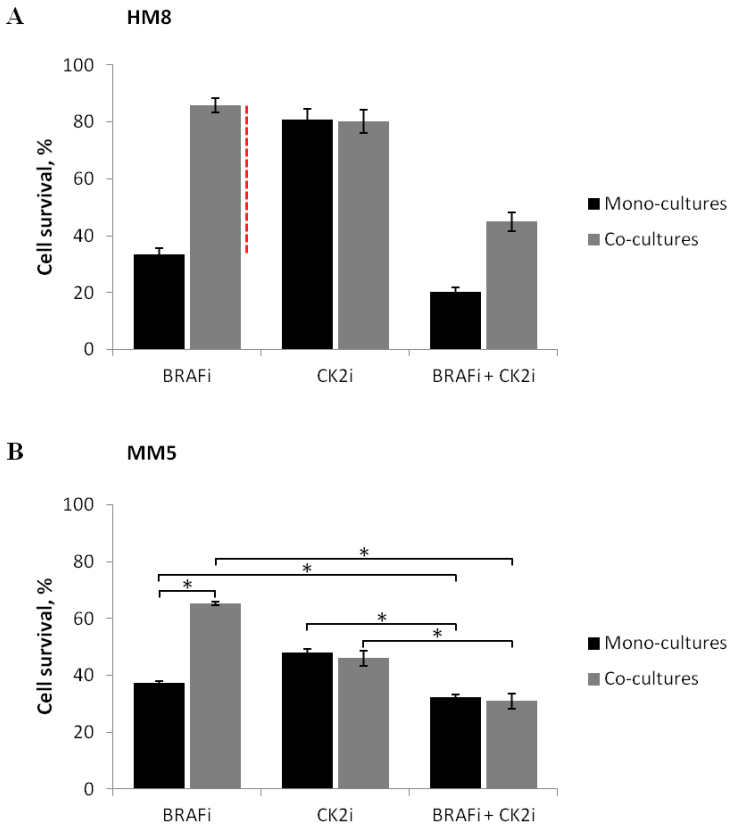

Figure 3.6: BRAF and CK2 inhibitors reduce the protective influence on the melanoma cells mediated by fibroblasts in co-cultures. The melanoma cells HM8 (A) and Melmet 5 (B) were grown as mono-cultures or co-cultures with lung fibroblasts WI-38 and treated with/without 0,5 µM BRAFi and 7,5 µM CK2i for 72 h. The red dotted line represents the fibroblast-mediated protection. The cell viability effect on selected cells was scored by measuring bioluminescence and is presented as % relative to the non-treated controls. Error bars indicate st.dev. from 3 technical parallels for HM8 cell line (A) and average ± SEM, $n \geq 3$, for Melmet 5 cell line (B). *, p-value < 0,05, unpaired t-test.

The protection induced by the stromal cells was significantly reduced in the HM8 cell line and completely abolished in the Melmet 5 cell line when combination treatment with BRAFi and PI3Ki was used on co-cultures (Figure 3.7). The combination treatment on co-cultures was more effective in cell viability reduction, compared to BRAFi mono-treatment. However, it should be noted that mono-treatment with PI3Ki highly reduced cell viability in Melmet 5 cultures. The significant reduction in cell viability of Melmet 5 cultures can be explained by too high concentration of PI3Ki.

Overall, the fibroblasts-associated cancer cells' resistance to BRAFi in co-cultures was reduced with the combination treatment of BRAFi and PI3Ki for both melanoma cell lines.

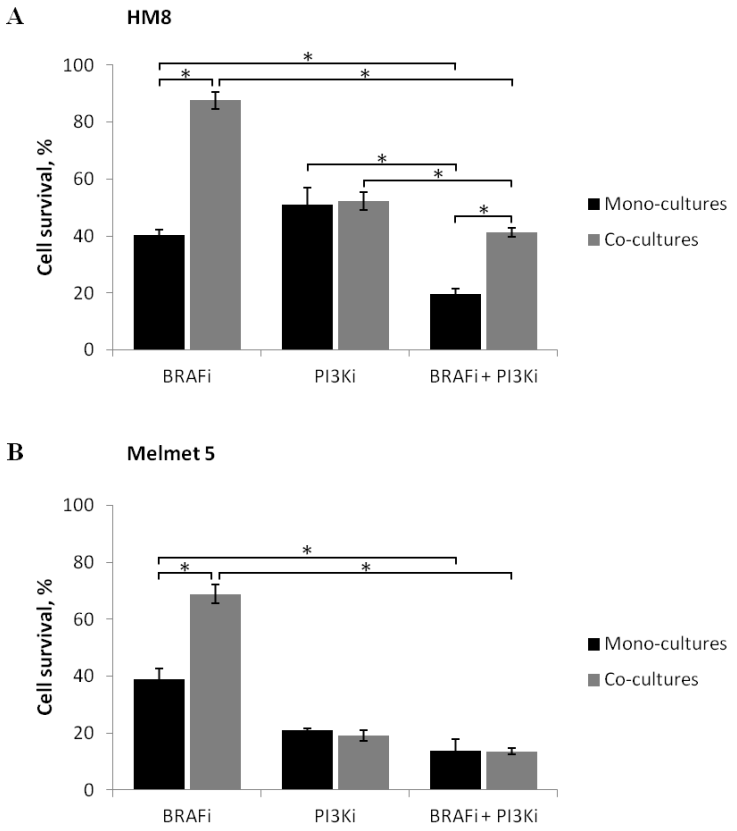

Figure 3.7: BRAF and PI3K inhibitors reduce the protective influence on the melanoma cells mediated by fibroblasts in co-cultures. The melanoma cells HM8 (A) and Melmet 5 (B) were grown as mono-cultures or co-cultures with lung fibroblasts WI-38 and treated with/without 0,5 µM BRAFi and 1 µM PI3Ki for 72 h. The cell viability effect on selected cells was scored by measuring bioluminescence and is presented as % relative to the non-treated controls (average ± SEM, n ≥ 3), *, p-value < 0,05, unpaired t-test.

The protection induced by the stromal cells in HM8 and Melmet 5 co-cultures was significantly reduced with the combination treatment of BRAFi and mTORi (Figure 3.8). In addition, the significant reduction in the cell viability was observed in both cell lines when the cultures were treated with the combination treatment, compared to mono-treatment with mTORi.

Altogether, the fibroblast-induced protection to BRAFi was significantly reduced in the HM8 cell line and eliminated in the Melmet 5 cell line when combination treatment with BRAFi and mTORi was used on co-cultures.

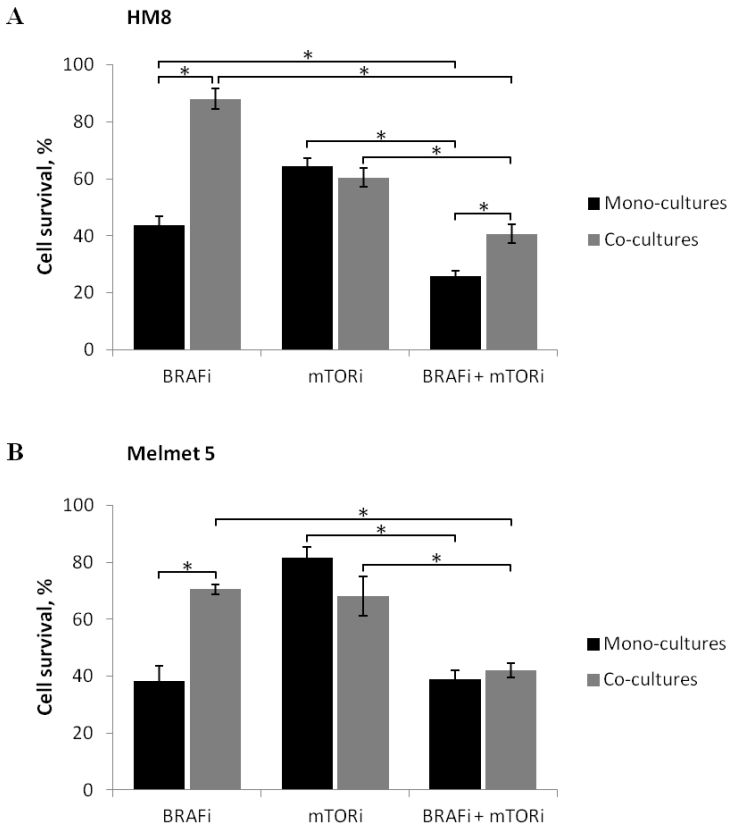

Figure 3.8: BRAF and mTOR inhibitors reduce the protective influence on the melanoma cells mediated by fibroblasts in co-cultures. The melanoma cells HM8 (A) and Melmet 5 (B) were grown as mono-cultures or co-cultures with lung fibroblasts and treated with/without 0,5 µM BRAFi and 5 nM mTORi for 72 h. The cell viability effect on selected cells was scored by measuring bioluminescence and is presented as % relative to the non-treated controls (average ± SEM, n ≥ 3), *, p-value < 0,05, unpaired t-test.

3.5. Protein expression in HM8 melanoma cells treated with BRAFi and CK2i combination treatment

To investigate the effect of BRAFi, CK2i or the combination of both targeted drugs at the protein level, HM8 cells were grown as mono-cultures and analysed for the levels of phospho-proteins pERK and pS6 indicative of activation in the MAPK/ERK and PI3K/AKT/mTOR pathways, respectively. Two different methods for protein analysis were applied: Western immunoblotting and Simple Western immunoassay.

3.5.1. Western immunoblotting for protein detection

The Western immunoblotting result demonstrated that the cancer cells without treatment (controls) have a high level of pERK (Thr202/204) (MAPK/ERK signaling pathway) and pS6 (Ser235/236) (PI3K/AKT/mTOR signaling pathway) (Figure 3.9). When the HM8 cells were treated with BRAFi, a reduction in phosphorylation of ERK and S6 was observed, indicating suppression of the MAPK/ERK and PI3K/AKT/mTOR signaling. No clear reduction in pERK level and some reduction in pS6 level were observed following mono-treatment with CK2i, compared to non-treated cells. The reduction in phosphorylation of ERK and S6 was most pronounced in cells exposed to the combination treatment of BRAFi and CK2i. Overall, the observed reduction in phospho-protein levels corresponded well with the cell viability reduction results obtained from the combination treatment on HM8 cells in Figure 3.6 A.

The levels of the total ERK and S6 proteins indicated equivalent amounts of these proteins in all samples. In addition, an antibody recognizing H3 was included as a protein loading (to validate equal loading).

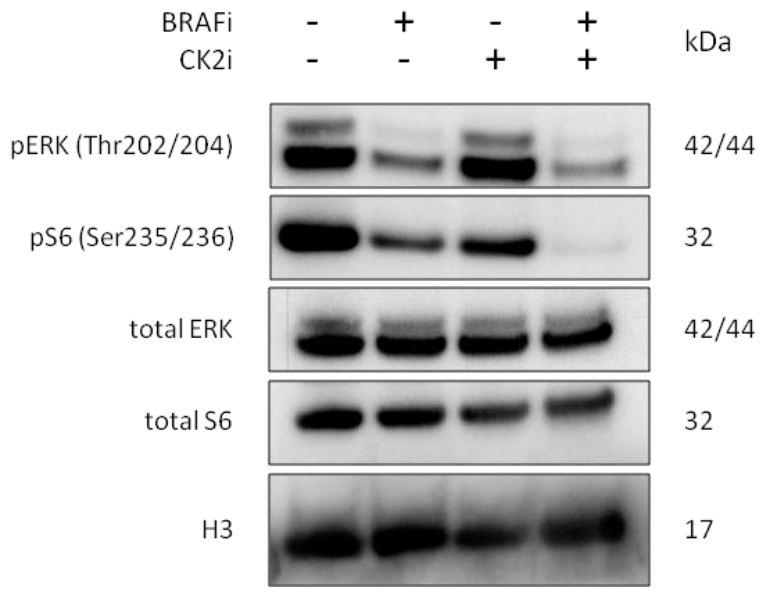

Figure 3.9: HM8 cell line grown as mono-culture show a good response to the combination treatment. Western immunoblotting analysis of the different proteins (H3 serves as a loading control) in non-treated or 24 h treated (0,5 µM BRAFi, 7,5 µM CK2i or their combination) melanoma cells.

3.5.2. Simple Western immunoassay for protein detection

The Simple Western immunoassay detected peaks at the right size for both pERK and pS6 (Figure 3.10). The HM8 cells treated with BRAFi showed a reduction of pERK and pS6 peaks heights. Mono-treatment with CK2i gave a small effect in protein levels reduction compared to non-treated controls. The main reduction in pERK and pS6 peaks was observed with the combination treatment of BRAFi and CK2i. β-actin was used as a loading control. β-actin levels indicated that equal amounts of proteins were loaded in all samples.

In order to determine the amounts of phospho-proteins detected by chemiluminescence from size-based Simple Western immunoassay, the area under the curve (AUC) of each sample was calculated by the corresponding software and the obtained values were normalized to β-actin controls (Figure 3.11).

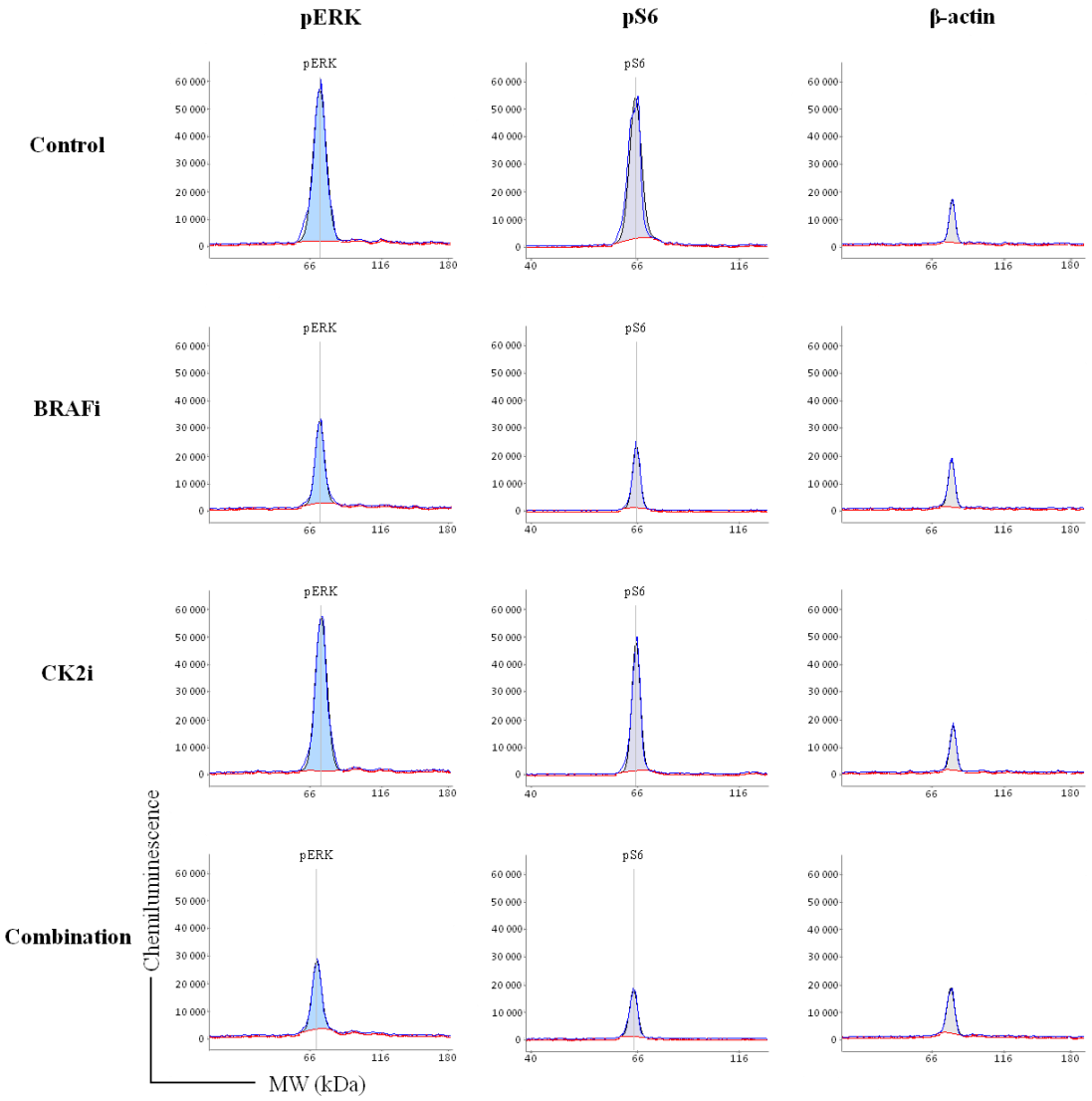

Figure 3.10: Representative measurements of pERK, pS6 and β-actin detected by size-based Simple Western immunoassay. HM8 melanoma cells were grown as mono-cultures and treated with 0,5 µM BRAFi, 7,5 µM CK2i or their combination for 48 h. The AUCs are illustrated with colours and represents the detected amounts of proteins. The y-axis indicates intensity of the chemiluminescence signal and the x-axis indicates protein size (kDa).

By setting the non-treated controls to 100%, it was calculated that pERK level decreased by 75% with the combination treatment of BRAFi and CK2i (Figure 3.11 A). However, the same reduction in pERK was also observed when BRAFi mono-treatment was used, meaning that the effect of combination treatment on pERK was primarily due to the BRAFi.

The level of pS6 was reduced by 90% with the combination treatment (Figure 3.11 B). However, the effect of combination treatment on pS6 was mainly due to BRAFi, since mono-treatment with the drug reduced pS6 level by 81%.

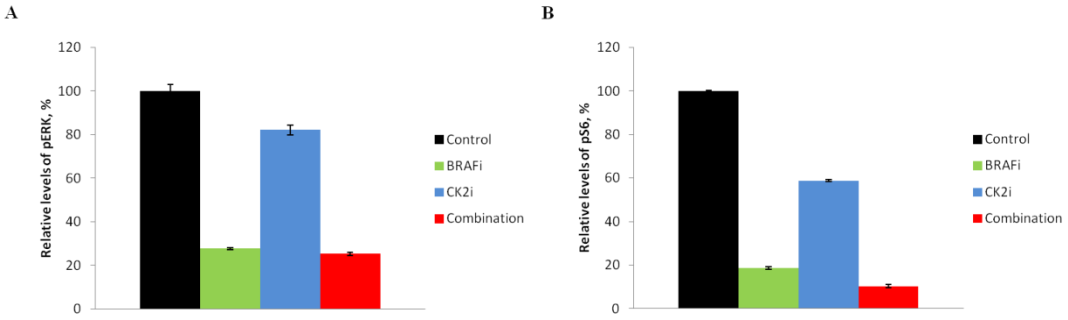

Figure 3.11: The levels of pERK and pS6 detected by Simple Western immunoassay. HM8 melanoma cells were grown as mono-cultures and treated with 0,5 µM BRAFi (green), 7,5 µM CK2i (blue) or their combination (red) for 48h. The levels of pERK (A) and pS6 (B) were calculated based on AUC. The results are presented as % relative to the non-treated controls (black). The y-axis indicates the relative levels of phospho-proteins and the x-axis indicates differently treated HM8 cells. Error bars indicate st.dev. from 2 biological replicates.

3.6. FLOW cytometry for phospho-protein detection

To explore the levels of phospho-proteins involved in the MAPK/ERK and PI3K/AKT/mTOR pathways in single melanoma cells, flow cytometry was used (Figure 3.12). The HM8 cells were grown as mono- and co-cultures with fibroblasts and treated with the BRAFi, CK2i or a combination of both drugs. Since melanoma cells were stably labeled with GFP-luciferase, we could separate GFP-positive cancer cells from the non-labeled stromal cells by flow cytometry and thereby analyze the protein levels in the melanoma cells from co-cultures. In addition, flow cytometry allows identification of distinct cell subpopulations based on the protein levels.

In the mono-cultures (Figure 3.12 A), we observed reduction in the levels of pERK and pS6 after the combination treatment (red lines in histograms), compared to non-treated control samples (black lines). The same reduction in pERK and pS6 levels was observed after BRAFi mono-treatment (green lines). The effect of CK2i on pS6 was notably lower, and no clear effect was observed on pERK (blue lines). This data is in line to the observations made by Western immunoblotting and Simple Western immunoassay on the mono-culture samples.

In the co-cultured melanoma cells (Figure 3.12 B), the effect of combination treatment and BRAFi mono-treatment was different. In BRAFi samples stained for pS6 we identified two cell populations (indicated in the second panel in Figure 3.12 B): one with clearly reduced pS6 levels, and the other with the high pS6 levels like in non-treated controls. In the samples

treated with the combination treatment, all the cells had low level of pS6. CK2i mono-treatment also efficiently reduced the levels of pS6. The pERK levels remained high in samples treated with CK2i. In contrast, the suppression of pERK was observed after BRAFi mono-treatment, and the level was further reduced in the combination treatment samples.

In conclusion, we observed that the combination treatment with BRAFi and CK2i was more effective in suppressing pERK and pS6 compared to BRAFi mono-treatment in the co-cultures. In the mono-cultures, however, BRAFi mono-treatment was an efficient approach to suppress pERK and pS6 and the combination treatment did not potentiate the effect.

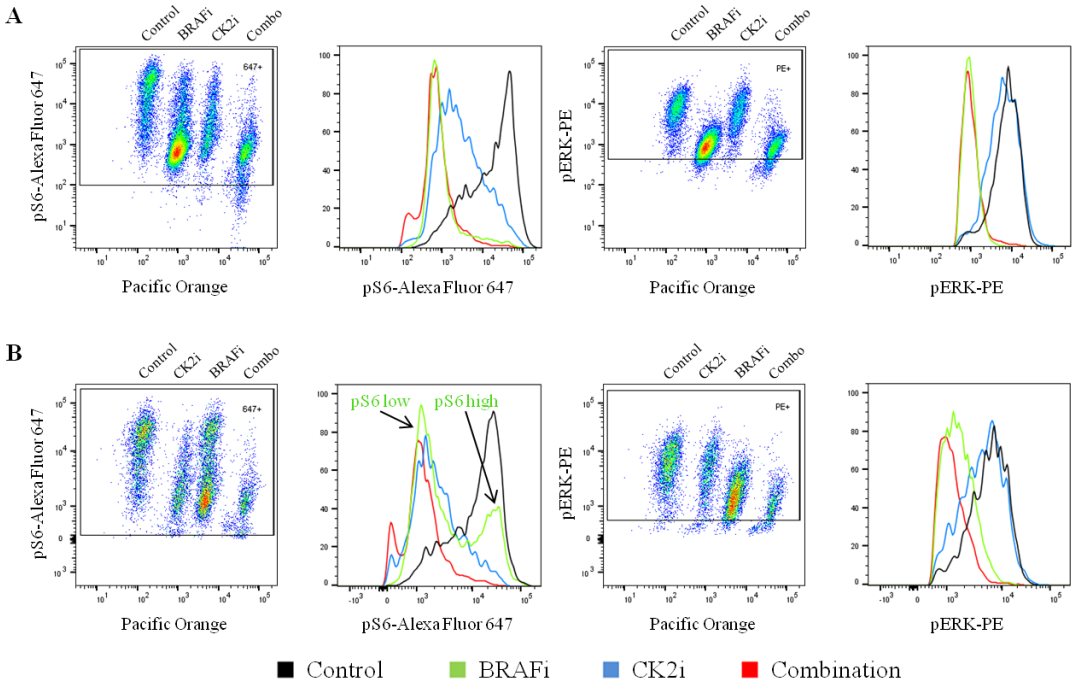

Figure 3.12: Flow cytometry analysis of phospho-protein levels in HM8 melanoma cell line in mono- and co-cultures. HM8 melanoma cells were grown as mono-cultures (A) or co-cultures with fibroblasts (B) and treated with 0,5 µM BRAFi (green), 7,5 µM CK2i (blue) or their combination (red) for 48 h. Non-treated control cells are shown in black. The data are shown as dot plots representing four differently treated samples (as indicated) or as color-coded histograms. By gating on the GFP signal, the tumor cells were separated from stromal cells, before further analysis for pS6 and pERK levels. To note, the sample order in the dot plots in A and B is different.

4. Discussion

The cancer associated fibroblasts (CAFs) induce protection in co-cultures treated with BRAFi mono-treatment. In this master project the melanoma cell lines HM8 and Melmet 5 were co-cultured with fibroblasts WI38. Combination of BRAFi and inhibitors targeting PI3K/AKT/mTOR pathway were investigated in order to examine possible elimination of the fibroblast-mediated protection to BRAFi. Furthermore, the levels of pERK and pS6 proteins in mono- and co-cultures were measured to find whether the combination treatment can effectively suppress the MAPK/ERK and PI3K/AKT/mTOR pathways, compared to BRAFi mono-treatment.

4.1. Stromal-mediated resistance to BRAFi treatment

The tumor-stromal functional interactions in the TME have an important role in tumor response to targeted therapy. This microenvironment-mediated resistance effect has been previously documented in several articles[79-81]. This resistance to BRAFi is a well known problem in the clinical treatment of patients with malignant melanoma and as reported by Straussman et al., stromal cells (e.g. fibroblasts) secrete factors that induce innate RAF-inhibitor mediated resistance to therapy[82].

In the present study, we observed that melanoma cell lines HM8 and Melmet 5 co-cultured with stromal cells, i.e. lung fibroblasts WI-38, had reduced sensitivity to BRAFi and fibroblast-mediated protection was observed during mono-treatment with this inhibitor. The obtained results confirmed previously reported observations by Seip et al.[83] in our group, demonstrating the CAFs ability to induce resistance to BRAFi. Such observed fibroblast-mediated resistance to BRAFi could be a result of reactivation of the MAPK/ERK pathway or activation of the alternative PI3K/AKT/mTOR signaling pathway in the cells[84], and this was further investigated through our study.

4.2. Combination treatment with MAPK/ERK and PI3K/AKT/mTOR pathway inhibitors

4.2.1. Mono-cultures treated with combination therapy

The results demonstrated that the combination treatment of mono-cultures was not more effective in reducing cell viability than mono-treatment with BRAFi. A possible explanation is that mono-cultured cells predominantly utilize the MAPK/ERK pathway and were therefore effectively inhibited with BRAFi.

4.2.2. Co-cultures treated with the combination treatment

The principal aim of the present study was to investigate whether combination therapy co-targeting multiple pathways within MAPK/ERK and PI3K/AKT/mTOR cascades could give beneficial response in treatment of BRAFi-resistant melanomas. Prior to this master project, a cancer drug sensitivity screening was performed by Dr. Kotryna Seip from the Dept. Tumor Biology group at the Norwegian Radium Hospital, where the CK2, involved in PI3K/AKT/mTOR pathway, was identified as a promising target. A CK2 inhibitor silmitasertib was thus selected for use in this project in combination with BRAFi to investigate whether the combined treatment could eliminate the stromal-mediated protective effect against BRAFi.

The combination treatment with BRAFi and CK2i was tested in co-cultures and we observed reduced proliferation in HM8 and Melmet 5 cell lines. A similar study was previously published by Chua et al., where the additional inhibition in proliferation of the BRAF mutant melanoma cell lines was seen when combining BRAFi with CK2i[32], compared to mono-treatment with BRAFi. This publication confirms our observations in co-cultures, demonstrating an improved effect in viability reduction and fibroblast-mediated resistance reduction in melanoma cells treated with the combination treatment.

Through the observations in this study we concluded that the protection induced by the stromal cells was reduced in the HM8 cell line and completely abolished in the Melmet 5 cell line when BRAFi was used in a combination with CK2i. This indicated that the combination

treatment was more effective in reduction of fibroblast-mediated protection than mono-treatment with BRAFi.

4.2.3. Other possible combination treatments

The activation of the alternative proliferation-inducing PI3K/AKT/mTOR signaling pathway has been proposed to be a mechanism of resistance against BRAFi[85]. The targeted CK2 is present (high) upstream of the PI3K/AKT/mTOR pathway, therefore it was interesting to also test other targeting drugs downstream of the PI3K/AKT/mTOR pathway. In order to evaluate whether targeting of the MAPK/ERK and PI3K/AKT/mTOR pathways, would eliminate protective resistance in melanoma cells, the PI3Ki and mTORi were used in combination with BRAFi.

We observed that combination treatment with BRAFi and PI3Ki improved the BRAFi effect on co-cultured melanoma cells by inducing a significant reduction in cell viability, compared to mono treatment with BRAFi. In HM8 and Melmet 5 cells the fibroblast-induced protection was completely eliminated with PI3Ki mono-treatment, suggesting that too high dose of this inhibitor might have been used in the experiment. This observation suggests that the PI3K, which is present lower downstream in the PI3K/AKT/mTOR pathway than CK2, has a better effect in reduction of the fibroblast-mediated resistance due to its position of targeting in the pathway. In addition, it is possible that the co-cultured cells prefer both MAPK/ERK and PI3K/AKT/mTOR signaling pathways and thereby were effectively repressed by both inhibitors. The last tested combination treatment involved BRAFi in combination with mTORi. This combination treatment has significantly reduced the stromal-mediated resistance to MAPK/ERK inhibitor in both HM8 and Melmet 5 cell lines. BRAFi in combination with mTORi had an equal effect in the cell viability reduction and the fibroblast-induced resistance effect reduction as the combination treatment using BRAFi and PI3Ki.

It has previously been published that by targeting multiple pathways, such as MAPK/ERK and PI3K/AKT/mTOR pathways, higher elimination of resistance to BRAF inhibitor is observed than by targeting a single pathway[86]. This was also confirmed with our study on co-cultures. In summary, our results demonstrated that fibroblast-mediated protection to BRAFi was significantly reduced or eliminated by combined drug targeted treatment with MAPK/ERK inhibitor (BRAFi) in combination with PI3K/AKT/mTOR pathway inhibitor (CK2i, PI3Ki or mTORi). The observed cell viability results from co-cultures indicated that

BRAFi in combination with CK2i, PI3Ki or mTORi had a much better effect in reducing the fibroblast-mediated protection than treatment with BRAFi. Therefore the combination treatment may be an effective treatment against the fibroblast-mediated protection to BRAFi. In addition, in all tested combination treatments, the co-cultured Melmet 5 cells were more sensitive to the combination treatment compared to the co-cultured HM8 cells.

4.3. Analysis of phospho-proteins involved in the MAPK/ERK and PI3K/AKT/mTOR pathways

In this part of the project, the phospho-protein levels were measured by using three various analytical techniques, Western immunoblotting, Simple Western immunoassay and flow cytometry, which may provide insight into response in HM8 cells to therapy with BRAFi, CK2i or the combination with both targeted drugs. We investigated whether the combination treatment targeting multiple pathways in mono- and co-cultures was more effective in reduction of phosphorylated proteins ERK and S6 levels than mono-treatment with BRAFi.

Western immunoblotting was performed on lysates from HM8 cell line grown as mono-cultures. These results verified that BRAFi mono-treatment suppressed the MAPK/ERK and to some extent PI3K/AKT/mTOR signaling cascades in mono-cultures and the cells were highly sensitive to BRAFi. No clear reduction in pERK level and a slight reduction in pS6 level was observed following mono-treatment with CK2i, indicating that the HM8 cells were less sensitive to this inhibitor. After combination treatment with both targeted drugs the protein levels were decreased, however, the reason for that may be that the BRAFi alone was effective in reducing protein levels.

Furthermore, mono-cultures were analysed by Simple Western immunoassay, and the obtained results also showed that BRAFi mono-treatment was effective in reduction of the pERK and pS6 protein levels in HM8 mono-cultured cells. The pERK protein level was high, while the pS6 protein level was slightly reduced, compared to non-treated controls, when mono-treatment with CK2i was used. HM8 cells were less sensitive to CK2 inhibitor. In the combination treatment with BRAFi and CK2i protein levels were reduced. However, the combination treatment induced reduction in protein levels was mostly affected by the effect of BRAFi, as previously observed with Western immunoblotting.

Flow cytometry analysis of phospho-protein levels in HM8 cell line in mono- and co-cultures, confirmed that downstream elements of the MAPK/ERK and the PI3K/AKT/mTOR signaling pathways (pERK and pS6, respectively) were reduced when targeted with BRAFi and CK2i. In mono-cultures the reduction of phospho-protein levels in the combination treatment was comparable to mono-treatment with BRAFi, as observed previously with other analytical techniques. In contrast, in co-cultures the combination treatment with BRAFi and CK2i had better effect than BRAFi mono-treatment. The levels of the downstream elements, pERK and pS6, were effectively suppressed in melanoma cells in the combination treatment compared to mono-treatments. Based on the pS6 protein level, cellular heterogeneity was observed (pS6 low and pS6 high), when treated with BRAFi mono-treatment. The possible reason for the high pS6 level might be the fibroblast-mediated protection to BRAFi in co-cultured cells. According to this finding, it is possible that the reactivation of the MAPK/ERK pathway or the activation of the alternative PI3K/AKT/mTOR pathway was present in the subpopulation of melanoma cells having high pS6 levels.

In summary, protein analysis demonstrated that the combination treatment with BRAFi and CK2i was effective in reducing the pERK and pS6 protein levels. However, the observed reduction in phospho-protein levels in mono-cultures was mostly affected by the effect of BRAFi. The fibroblast-mediated protection to BRAFi in co-cultured cells was decreased when co-inhibiting the MAPK/ERK and PI3K/AKT/mTOR signaling pathways. In co-cultures, the combination treatment with BRAFi and CK2i was more effective in suppressing pERK and pS6 protein levels than mono-treatment with BRAFi, suggesting that this combination of inhibitors might be an effective treatment for BRAF mutated melanomas.

4.4. Methodological discussion

4.4.1. Cell culture work

In this project, two metastatic melanoma cell lines HM8 and Melmet 5 were used for *in vitro* experiments, in addition to the fibroblast cell line WI-38. Different treatment methods were performed on the cell lines to investigate the cell viability responses to targeted drug therapy. Analysis of treatment with targeted drugs on mono-cultures is not a good representative model since *in vivo* the cells are highly affected by the tumor microenvironment. The co-cultures were established as a model that imitates better the micro environmental

surroundings of an organism (when exposed to drug therapy) and mimic response seen in patients.

4.4.2. Protein analysis

Simple Western immunoassay technique allowed us to significantly reduce the amounts of protein lysates needed for the protein analysis, which was remarkably less compared to classical protein detection method, Western immunoblotting. In addition, Simple Western immunoassay was a more quantitative technique compared to Western immunoblotting protein analysis.

On Western immunoblotting and Simple Western immunoassay only mono-cultures were analysed, co-cultures needed to be sorted by fluorescence-activated cell sorting (FACS) to analyze the protein levels deriving from melanoma cells only. In addition, the FACS technique used for cell isolation requires a large amounts of cells[87]. Flow cytometry was used for analysis of co-cultures, where the GFP-positive cancer cells were separated from the GFP-negative stromal cells by gating on the GFP signal. This technique allowed observation of cellular heterogeneity based on the protein levels.

Taken all together, Western immunoblotting, Simple Western immunoassay and flow cytometry results were highly comparable and indicated that all three techniques could be used interchangeable for the protein analysis on mono-cultures. Flow cytometry technique provided an advantage when it came to analyzing co-cultures, where the protein levels in melanoma cells were detectable after the separation of the GFP-positive and GFP-negative cells in co-cultures.

5. Concluding remarks

Metastatic melanoma is an aggressive type of skin cancer[50] showing high resistance to treatment. Targeted therapy with BRAFi has shown improved clinical responses in melanoma patients. However, the therapeutic benefit is limited due to development resistance. Tumor microenvironment including stromal cells was shown to be able to facilitate BRAFi resistance. In this master project we have demonstrated that:

- The presence of fibroblasts reduced sensitivity to BRAFi in melanoma cells grown in co-cultures, indicating fibroblast-mediated protection from the drug.
- The fibroblast-mediated protection was reduced in HM8 and eliminated in Melmet 5 melanoma cells when BRAFi treatment was combined with PI3K/AKT/mTOR pathway inhibitors, CK2i, PI3Ki or mTORi.
- In the mono-cultures, levels of pERK and pS6 were strongly reduced by BRAFi, indicating an effective suppression of the MAPK/ERK and PI3K/AKT/mTOR pathways. The levels of pERK and pS6 were not further reduced with the combination treatment of BRAFi and CK2i, indicating that addition of CK2i did not potentiate the suppressive effect of BRAFi in the mono-cultures.
- In the co-cultures, the levels of pERK and pS6 proteins were reduced by BRAFi. However, the remaining pERK and pS6 levels were higher than in BRAFi-treated mono-cultures, indicating lower effect of BRAFi in the co-cultures. The level of pERK and pS6 was further reduced with the combination treatment of BRAFi and CK2i, indicating a more effective suppression of the MAPK/ERK and PI3K/AKT/mTOR pathways.

Taken all together, the demonstrated data suggests that the combination treatment with BRAFi and CK2i might potentiate treatment effect in melanoma cells protected by fibroblasts. The combination of BRAFi with PI3K/AKT/mTOR pathway inhibitors might also be an attractive alternative for improvement of therapeutic benefit when treating stroma-rich melanoma tumors.

6. Future perspectives

In the light of our observations, we suggest that:

- The importance of the tumor microenvironment in cancer development, progression and mediated resistance and its interactions with melanoma cells should be further thoroughly investigated.

- Additional studies are required for better understanding of the resistance mechanisms against BRAFi in melanoma patients.

- The combination treatment effect could be further evaluated in *in vivo* models, for better understanding of the resistance mechanisms against BRAFi.

- A future study of CK2 pathway is important to clarify whether and how this pathway is involved in the other cancer related cascades and stromal-mediated resistance.

- The identification of other possible targets in MAPK/ERK and PI3K/AKT/mTOR pathways, or other cancer associated pathways, should be investigated due to the promising effects of the combination therapies targeting multiple pathways and thus potential for improvement of current treatment strategies in the clinic.

Supplementary Table: Materials

General cell work/cell culturing	Company	Catalogue number
RPMI-1640 medium	Sigma-Aldrich, St. Louis, MO	R0883
EMEM medium	ATCC, Manassas, VA	30-2003
Fetal Bovine Serum (FBS)	Sigma-Aldrich, St. Louis, MO	F7524
L-alanyl-L-glutamine	Sigma-Aldrich, St. Louis, MO	G8541
Dulbecco's Phosphate Buffered Saline (PBS)	Sigma-Aldrich, St. Louis, MO	D8537
Ethylenediaminetetraacetic acid solution (EDTA)	Sigma-Aldrich, St. Louis, MO	E8008
Trypsin-EDTA solution (1X)	Sigma-Aldrich, St. Louis, MO	T3924
Trypan Blue Stain (0,4%)	NanoEnTek Inc., Guro-gu, Seoul, Korea	EBT-001
Countess™ cell counting chamber slides	Thermo Fisher Scientific, Waltham, MA	C10228
Dimethyl Sulfoxide (DMSO)	Sigma-Aldrich, St. Louis, MO	D2650
96-Well White Clear-Bottom Plates	Costar, Corning, NY	3610
Nunc™ EasYFlasks™ Cell Culture Flasks, 75 cm^2	Thermo Fisher Scientific, Waltham, MA	156499
Nunc™ EasYFlasks™ Cell Culture Flasks, 25 cm^2	Thermo Fisher Scientific, Waltham, MA	156367
D-Luciferin	Biosynth AG, Staad, Switzerland	L-8220

Therapeutic drugs	Company	Catalogue number
Vemurafenib (BRAFi)	Selleck Chemicals, Houston, TX	S1267
Silmitasertib (CK2i)	Selleck Chemicals, Houston, TX	S2248
Buparlisib (PI3Ki)	Selleck Chemicals, Houston, TX	S2247
Everolimus (mTORi)	Novartis, Basel, Switzerland	07741

Western Blotting	Company	Catalogue number
Pierce™ BCA Protein Assay Kit	Thermo Scientific, Rockford, IL	23227
NuPAGE™ 4-12% Bis-Tris 1,0 mm 12 well gel	Invitrogen™, Carlsbad, CA	NP0323BOX
NuPAGE™ MES SDS Running Buffer (20X)	Invitrogen™, Carlsbad, CA	NP000202
NuPAGE™ LDS Sample Buffer (4X)	Invitrogen™, Carlsbad, CA	NP0008
Polyvinylidene difluoride (PVDF) membrane and Chromatography Paper Sheet	Whatman™, Maidstone, UK	3030-335
Methanol	VWR Chemicals, Radnor, PA	20847.307
SeeBlue™ Pre-stained Protein Standard	Invitrogen™, Carlsbad, CA	LC5625
SuperSignal™ West Dura Extended Duration Substrate	Thermo Scientific, Rockford, IL	A34076F
Protease inhibitor (cOmplete)	Roche Applied Science, Mannheim, Germany	04693124001
Phosphatase inhibitor (PhosSTOP)	Roche Applied Science, Mannheim, Germany	04906837001
XCell SureLock™ Mini-Cell	Thermo Fisher Scientific, Waltham, MA	EI0002
XCell II™ Blot Module	Thermo Fisher Scientific, Waltham, MA	EI9051

Simple Western	Company	Catalogue number
12-230 kDa Peggy Sue Separation Module	Protein Simple, San Jose, CA	SM-S001
Anti-Rabbit Detection Module	Protein Simple, San Jose, CA	DM-001
Anti-Mouse Detection Module	Protein Simple, San Jose, CA	DM-002

Flow cytometry	Company	Catalogue number
Pacific Orange™ dye	Invitrogen™, Carlsbad, CA	S32365
Pacific Blue™ dye	Invitrogen™, Carlsbad, CA	A35122
Bovine Serum Albumin (BSA)	Roche Applied Science, Mannheim, Germany	10735086001

Antibodies for Western blotting, Simple Western system and Flow	Company	Catalogue number
Anti-p44/42 MAPK (Thr202/Tyr204)	Cell Signaling Technology, Danvers, MA	4370
Anti-pS6 (Ser235/236)	Cell Signaling Technology, Danvers, MA	4858
p44/42 MAPK (Erk1/2)	Cell Signaling Technology, Danvers, MA	4695
S6	Cell Signaling Technology, Danvers, MA	2217
Anti-Rabbit Immunoglobulins/HRP	Dako Denmark A/S, Glostrup, Denmark	P0448
Anti- Mouse Immunoglobulins/HRP	Dako Denmark A/S, Glostrup, Denmark	P0260
Anti-pERK-PE	Cell Signaling Technology, Danvers, MA	14095
Anti-pS6-Alexa Fluor 647	Cell Signaling Technology, Danvers, MA	4851
Histone H3	Cell Signaling Technology, Danvers, MA	4499
Anti β-actin	Sigma-Aldrich, St. Louis, MO	A5316

Instrument/machine	Company	Catalogue number	Software
Countess™ II Automated Cell Counter	Thermo Fisher Scientific, Waltham, MA	AMQAX1000	
Victor™ *X*3 Multimode plate reader	Perkin Elmer, Waltham, MA	2030-0050	
CKX41 inverted microscope	Olympus, Waltham, MA	CKX41	
ROTINA 420 centrifuge	Hettich, Tuttlingen, Germany	Z723630	
Digital Multi Heat Block	VWR, Radnor, PA	13259-056	
G:Box instrument	Syngene, Cambridge, UK		GeneSnap
Peggy Sue™	Protein Simple, San Jose, CA		Compass
LSR II FLOW cytometer	BD Bioscience, San Jose, CA		FlowJo

Supplementary Table: Buffers

Lysis buffer	
Triton X-100	1 %
HEPES (pH 7,4, 1M)	0,05 M
NaCl (Sodium chloride)	0,15 M
$MgCl_2$	0,0015 M
EGTA	0,001 M
NaF	0,1 M
NaPyrophosphate	0,01 M
Na_3VO_4 (Sodium orthovanadate)	0,001 M
Glycerol	10 %

Transfer buffer	
Tris	3 g
Glycin	14,4 g
Methanol (MeOH)	200 mL
H_2O	800 mL

TBST buffer	
Tris-HCl	1 M
NaCl	5 M
Tween-20	5 mL
H_2O	945 mL

References

1. Pecorino, L., *Molecular Biology of Cancer*. Third ed. 2012: Oxford University Press. 342.
2. WorldHealthOrganization, *http://www.who.int/cancer/en/*. 2016(Accessed 19'th of March, 2018).
3. CancerRegistryofNorway, *Cancer in Norway 2016 - Cancer incidence, mortality, survival and prevalence in Norway*. Cancer Registry of Norway, 2017(Accessed 19'th of March, 2018).
4. Danaei, G., et al., *Causes of cancer in the world: comparative risk assessment of nine behavioural and environmental risk factors*. The Lancet, 2005. **366**(9499): p. 1784-1793.
5. Hanahan, D. and Robert A. Weinberg, *Hallmarks of Cancer: The Next Generation*. Cell, 2011. **144**(5): p. 646-674.
6. Chial, H., *Tumor suppressor (TS) genes and the two-hit hypothesis*. Nature Education, 2008. **1**(1): p. 177.
7. Vogelstein, B., et al., *Cancer Genome Landscapes*. Science, 2013. **339**(6127): p. 1546-1558.
8. Vogelstein, B. and K.W. Kinzler, *Cancer genes and the pathways they control*. Nature Medicine, 2004. **10**: p. 789.
9. Giuseppina, G.M. and S. Alain, *TP53 mutations in human skin cancers*. Human Mutation, 2003. **21**(3): p. 217-228.
10. Oikonomou, E., et al., *BRAF vs RAS oncogenes: are mutations of the same pathway equal? differential signalling and therapeutic implications*. Oncotarget, 2014. **5**(23): p. 11752-11777.
11. Ascierto, P.A., et al., *The role of BRAF V600 mutation in melanoma*. Journal of Translational Medicine, 2012. **10**: p. 85-85.
12. Lodish, H., et al., *Molecular Cell Biology*. 4th ed. Section 24.2, Proto-Oncogenes and Tumor-Suppressor Genes. 2000: New York: W. H. Freeman.
13. Gupta, G.P. and J. Massagué, *Cancer Metastasis: Building a Framework*. Cell, 2006. **127**(4): p. 679-695.
14. Hunter, K.W., N.P.S. Crawford, and J. Alsarraj, *Mechanisms of metastasis*. Breast Cancer Research : BCR, 2008. **10**(Suppl 1): p. S2-S2.
15. Chambers, A.F., A.C. Groom, and I.C. MacDonald, *Dissemination and growth of cancer cells in metastatic sites*. Nature Reviews Cancer, 2002. **2**: p. 563.
16. Kircher, D.A., et al., *Melanoma Brain Metastasis: Mechanisms, Models, and Medicine*. International Journal of Molecular Sciences, 2016. **17**(9): p. 1468.
17. Valastyan, S. and Robert A. Weinberg, *Tumor Metastasis: Molecular Insights and Evolving Paradigms*. Cell, 2011. **147**(2): p. 275-292.
18. Lambert, A.W., D.R. Pattabiraman, and R.A. Weinberg, *Emerging Biological Principles of Metastasis*. Cell, 2017. **168**(4): p. 670-691.
19. Massagué, J. and A.C. Obenauf, *Metastatic colonization by circulating tumour cells*. Nature, 2016. **529**: p. 298.
20. Psaila, B. and D. Lyden, *The metastatic niche: adapting the foreign soil*. Nat Rev Cancer, 2009. **9**(4): p. 285-93.
21. Minn, A.J., et al., *Distinct organ-specific metastatic potential of individual breast cancer cells and primary tumors*. Journal of Clinical Investigation, 2005. **115**(1): p. 44-55.
22. Patel, J.K., et al., *Metastatic pattern of malignant melanoma: A study of 216 autopsy cases*. The American Journal of Surgery, 1978. **135**(6): p. 807-810.
23. Lopez-Bergami, P., B. Fitchman, and Z.e. Ronai, *Understanding Signaling Cascades in Melanoma*. Photochemistry and photobiology, 2008. **84**(2): p. 289-306.
24. Panka, D.J., M.B. Atkins, and J.W. Mier, *Targeting the Mitogen-Activated Protein Kinase Pathway in the Treatment of Malignant Melanoma*. Clinical Cancer Research, 2006. **12**(7): p. 2371s-2375s.
25. Pópulo, H., J.M. Lopes, and P. Soares, *The mTOR Signalling Pathway in Human Cancer*. International Journal of Molecular Sciences, 2012. **13**(2): p. 1886-1918.
26. Inamdar, G.S., S.V. Madhunapantula, and G.P. Robertson, *Targeting the MAPK Pathway in Melanoma: Why some approaches succeed and other fail*. Biochemical pharmacology, 2010. **80**(5): p. 624-637.
27. McCain, J., *The MAPK (ERK) Pathway: Investigational Combinations for the Treatment Of BRAF-Mutated Metastatic Melanoma*. Pharmacy and Therapeutics, 2013. **38**(2): p. 96-108.
28. Kwong, L.N. and M.A. Davies, *Navigating the Therapeutic Complexity of PI3K Pathway Inhibition in Melanoma*. Clinical cancer research : an official journal of the American Association for Cancer Research, 2013. **19**(19): p. 10.1158/1078-0432.CCR-13-0142.

29. Kim, L.C., R.S. Cook, and J. Chen, *mTORC1 and mTORC2 in cancer and the tumor microenvironment.* Oncogene, 2017. **36**(16): p. 2191-2201.
30. Liu, P., et al., *Targeting the phosphoinositide 3-kinase (PI3K) pathway in cancer.* Nature reviews. Drug discovery, 2009. **8**(8): p. 627-644.
31. Karbowniczek, M., et al., *mTOR Is Activated in the Majority of Malignant Melanomas.* Journal of Investigative Dermatology, 2008. **128**(4): p. 980-987.
32. Chua, M.M.J., et al., *CK2 in Cancer: Cellular and Biochemical Mechanisms and Potential Therapeutic Target.* Pharmaceuticals, 2017. **10**(1): p. 18.
33. Nuñez de Villavicencio-Diaz, T., A.J. Rabalski, and D.W. Litchfield, *Protein Kinase CK2: Intricate Relationships within Regulatory Cellular Networks.* Pharmaceuticals, 2017. **10**(1): p. 27.
34. Ortega, C.E., Y. Seidner, and I. Dominguez, *Mining CK2 in Cancer.* PLoS ONE, 2014. **9**(12): p. e115609.
35. Buontempo, F., et al., *Therapeutic targeting of CK2 in acute and chronic leukemias.* Leukemia, 2018. **32**(1): p. 1-10.
36. Zhou, B., et al., *Protein Kinase CK2α Maintains Extracellular Signal-regulated Kinase (ERK) Activity in a CK2α Kinase-independent Manner to Promote Resistance to Inhibitors of RAF and MEK but Not ERK in BRAF Mutant Melanoma.* The Journal of Biological Chemistry, 2016. **291**(34): p. 17804-17815.
37. Chen, F., et al., *New horizons in tumor microenvironment biology: challenges and opportunities.* BMC Medicine, 2015. **13**: p. 45.
38. Wang, M., et al., *Role of tumor microenvironment in tumorigenesis.* Journal of Cancer, 2017. **8**(5): p. 761-773.
39. Sounni, N.E. and A. Noel, *Targeting the Tumor Microenvironment for Cancer Therapy.* Clinical Chemistry, 2013. **59**(1): p. 85-93.
40. Hui, L. and Y. Chen, *Tumor microenvironment: Sanctuary of the devil.* Cancer Letters, 2015. **368**(1): p. 7-13.
41. Hanahan, D. and Lisa M. Coussens, *Accessories to the Crime: Functions of Cells Recruited to the Tumor Microenvironment.* Cancer Cell, 2012. **21**(3): p. 309-322.
42. Klemm, F. and J.A. Joyce, *Microenvironmental regulation of therapeutic response in cancer.* Trends in Cell Biology, 2015. **25**(4): p. 198-213.
43. Öhlund, D., E. Elyada, and D. Tuveson, *Fibroblast heterogeneity in the cancer wound.* The Journal of Experimental Medicine, 2014. **211**(8): p. 1503-1523.
44. Shiga, K., et al., *Cancer-Associated Fibroblasts: Their Characteristics and Their Roles in Tumor Growth.* Cancers, 2015. **7**(4): p. 2443-2458.
45. Tao, L., et al., *Cancer associated fibroblasts: An essential role in the tumor microenvironment.* Oncology Letters, 2017. **14**(3): p. 2611-2620.
46. Yamamura, Y., et al., *Akt–Girdin Signaling in Cancer-Associated Fibroblasts Contributes to Tumor Progression.* Cancer Research, 2015. **75**(5): p. 813-823.
47. Kalluri, R. and M. Zeisberg, *Fibroblasts in cancer.* Nature Reviews Cancer, 2006. **6**: p. 392.
48. Erdogan, B. and D.J. Webb, *Cancer-associated fibroblasts modulate growth factor signaling and extracellular matrix remodeling to regulate tumor metastasis.* Biochemical Society transactions, 2017. **45**(1): p. 229-236.
49. Vong, S. and R. Kalluri, *The Role of Stromal Myofibroblast and Extracellular Matrix in Tumor Angiogenesis.* Genes & Cancer, 2011. **2**(12): p. 1139-1145.
50. Uong, A. and L.I. Zon, *Melanocytes in Development and Cancer.* Journal of cellular physiology, 2010. **222**(1): p. 38-41.
51. Cichorek, M., et al., *Skin melanocytes: biology and development.* Advances in Dermatology and Allergology/Postępy Dermatologii I Alergologii, 2013. **30**(1): p. 30-41.
52. Denat, L., et al., *Melanocytes as Instigators and Victims of Oxidative Stress.* The Journal of investigative dermatology, 2014. **134**(6): p. 1512-1518.
53. Houghton, A.N. and D. Polsky, *Focus on melanoma.* Cancer Cell, 2002. **2**(4): p. 275-278.
54. RASTRELLI, M., et al., *Melanoma: Epidemiology, Risk Factors, Pathogenesis, Diagnosis and Classification.* In Vivo, 2014. **28**(6): p. 1005-1011.
55. Tryggvadóttir, L., et al., *Trends in the survival of patients diagnosed with malignant melanoma of the skin in the Nordic countries 1964–2003 followed up to the end of 2006.* Acta Oncologica, 2010. **49**(5): p. 665-672.
56. McCourt, C., O. Dolan, and G. Gormley, *Malignant Melanoma: A Pictorial Review.* The Ulster Medical Journal, 2014. **83**(2): p. 103-110.
57. Soura, E., et al., *Hereditary Melanoma: Update on Syndromes and Management - Genetics of familial atypical multiple mole melanoma syndrome.* Journal of the American Academy of Dermatology, 2016. **74**(3): p. 395-407.

58. E., G.J., et al., *Melanoma staging: Evidence-based changes in the American Joint Committee on Cancer eighth edition cancer staging manual*. CA: A Cancer Journal for Clinicians, 2017. **67**(6): p. 472-492.
59. Wisco, O.J. and A.J. Sober, *Prognostic Factors for Melanoma*. Dermatologic Clinics, 2012. **30**(3): p. 469-485.
60. Mohr, P., et al., *Staging of cutaneous melanoma*. Annals of Oncology, 2009. **20**(Suppl 6): p. vi14-vi21.
61. Miller, A.J. and M.C. Mihm, *Melanoma*. New England Journal of Medicine, 2006. **355**(1): p. 51-65.
62. Y., R.B., M.D. M., and T. Hensin, *Somatic driver mutations in melanoma*. Cancer, 2017. **123**(S11): p. 2104-2117.
63. Manzano, J.L., et al., *Resistant mechanisms to BRAF inhibitors in melanoma*. Annals of Translational Medicine, 2016. **4**(12): p. 237.
64. Wong, C.W., et al., *BRAF and NRAS mutations are uncommon in melanomas arising in diverse internal organs*. Journal of Clinical Pathology, 2005. **58**(6): p. 640-644.
65. Davies, H., et al., *Mutations of the BRAF gene in human cancer*. Nature, 2002. **417**: p. 949.
66. Leong, S.P.L., et al., *Progression of cutaneous melanoma: implications for treatment*. Clinical & experimental metastasis, 2012. **29**(7): p. 775-796.
67. Sosman, J.A., et al., *Survival in BRAF V600–Mutant Advanced Melanoma Treated with Vemurafenib*. The New England journal of medicine, 2012. **366**(8): p. 707-714.
68. Puzanov, I., P. Burnett, and K.T. Flaherty, *Biological challenges of BRAF inhibitor therapy*. Molecular Oncology, 2011. **5**(2): p. 116-123.
69. TANG, T., R. ELDABAJE, and L. YANG, *Current Status of Biological Therapies for the Treatment of Metastatic Melanoma*. Anticancer Research, 2016. **36**(7): p. 3229-3241.
70. Thakur, M.D. and D.D. Stuart, *The Evolution of Melanoma Resistance Reveals Therapeutic Opportunities*. Cancer Research, 2013. **73**(20): p. 6106-6110.
71. Fedorenko, I.V., K.H.T. Paraiso, and K.S.M. Smalley, *Acquired and intrinsic BRAF inhibitor resistance in BRAF V600E mutant melanoma*. Biochemical pharmacology, 2011. **82**(3): p. 201-209.
72. Paraiso, K.H.T., et al., *PTEN loss confers BRAF inhibitor resistance to melanoma cells through the suppression of BIM expression*. Cancer research, 2011. **71**(7): p. 2750-2760.
73. Kim, A. and M.S. Cohen, *The discovery of vemurafenib for the treatment of BRAF-mutated metastatic melanoma*. Expert opinion on drug discovery, 2016. **11**(9): p. 907-916.
74. Shi, H., et al., *Acquired resistance and clonal evolution in melanoma during BRAF inhibitor therapy*. Cancer discovery, 2014. **4**(1): p. 80-93.
75. Chapman, P.B., et al., *Improved Survival with Vemurafenib in Melanoma with BRAF V600E Mutation*. The New England journal of medicine, 2011. **364**(26): p. 2507-2516.
76. Palmieri, G., et al., *Multiple Molecular Pathways in Melanomagenesis: Characterization of Therapeutic Targets*. Frontiers in Oncology, 2015. **5**: p. 183.
77. Puzanov, I., et al., *Long-term outcome in BRAF(V600E) melanoma patients treated with vemurafenib: Patterns of disease progression and clinical management of limited progression*. European journal of cancer (Oxford, England : 1990), 2015. **51**(11): p. 1435-1443.
78. Seip, K., et al., *Fibroblast-induced switching to the mesenchymal-like phenotype and PI3K/mTOR signaling protects melanoma cells from BRAF inhibitors*. Oncotarget, 2016. **7**(15): p. 19997-20015.
79. Wang, W., et al., *Crosstalk to Stromal Fibroblasts Induces Resistance of Lung Cancer to Epidermal Growth Factor Receptor Tyrosine Kinase Inhibitors*. Clinical Cancer Research, 2009. **15**(21): p. 6630-6638.
80. Shekhar, M.P.V., et al., *Direct Involvement of Breast Tumor Fibroblasts in the Modulation of Tamoxifen Sensitivity*. The American Journal of Pathology, 2007. **170**(5): p. 1546-1560.
81. Shekhar, M.P.V., et al., *Breast Stroma Plays a Dominant Regulatory Role in Breast Epithelial Growth and Differentiation: Implications for Tumor Development and Progression*. Cancer Research, 2001. **61**(4): p. 1320-1326.
82. Straussman, R., et al., *Tumor microenvironment induces innate RAF-inhibitor resistance through HGF secretion*. Nature, 2012. **487**(7408): p. 500-504.
83. Seip, K., et al., *Targeting stroma-supported melanoma cells resistant to BRAF inhibitors*. Cancer Research, 2017.
84. Acciardo, S., et al., *Imaging markers of response to combined BRAF and MEK inhibition in BRAF mutated vemurafenib-sensitive and resistant melanomas*. Oncotarget, 2018. **9**(24): p. 16832-16846.
85. Chan, X.Y., et al., *Role Played by Signalling Pathways in Overcoming BRAF Inhibitor Resistance in Melanoma*. International Journal of Molecular Sciences, 2017. **18**(7): p. 1527.
86. Spagnolo, F., P. Ghiorzo, and P. Queirolo, *Overcoming resistance to BRAF inhibition in BRAF-mutated metastatic melanoma*. Oncotarget, 2014. **5**(21): p. 10206-10221.
87. Hu, P., et al., *Single Cell Isolation and Analysis*. Frontiers in Cell and Developmental Biology, 2016. **4**: p. 116.